NASA Contractor Report 178418

Consistent Linearization of the Element-Independent Corotational Formulation for the Structural Analysis of General Shells

C. C. Rankin

LOCKHEED PALO ALTO RESEARCH LABORATORY
PALO ALTO, CALIFORNIA 94304, USA

CONTRACT NAS1-18101
TASK 5

JANUARY 1988

National Aeronautics and
Space Administration

Langley Research Center
Hampton, Virginia 23665-5225

RoC.
11-9-88

November 7, 1988

Thelma,

Joan Swann called from JPL about a Langley document CR-178418, Accession number 88N17078. The CR printed on the document is 278428. Looks like the Langley printer liked the number 2 insread of the number 1. I will call Langley on this if there is more than just a number change to be amade on the document.

Trench

END OF I P S DOCUMENT # 159559

****

ABSTRACT

A consistent linearization is provided for the element-independent corotational formulation, providing the proper first and second variation of the strain energy. As a result, the *warping* problem that has plagued flat elements has been overcome, with beneficial effects carried over to *linear* solutions. True Newton quadratic convergence has been restored to the Structural Analysis of General Shells (STAGS) code for conservative loading using the full corotational implementation. Some implications for general finite element analysis are discussed, including what effect the automatic frame invariance provided by this work might have on the development of new, improved elements.

Table of Contents

Table of Contents (continued)

1. *Introduction*

In this report, the problem of element warping and slow, irregular convergence to nonlinear solution states will be addressed in the context of the element-independent corotational theory [7] now implemented in STAGS. We shall show that some of these results have implications beyond the original confines of the theory, and beyond the SH410 elements that were used in this investigation. Section 2 addresses the problems encountered during a linear analysis related to *warping*, and Section 3 addresses questions of *convergence* to nonlinear solutions.

2. *The Problem of Warping*

Many cases have surfaced where the normally reliable workhorse SH410 (410 for short) shell element has failed to produce a converged solution even for very fine grids. Perhaps the worst case of all is the large class of problems involving a doubly-curved surface, or in fact any curved surface for which *the nodes do not coincide with the surface.* Even though the finite element codes calculate the actual nodal coordinates, only the projected nodal positions on the plane formed by the element can be used in the element calculations: the 410 is a *flat plate* element. For the vast majority of cylinder, annulus, and even the sphere problem with the usual polar grid, the element plate sections properly tile the surface and difficulties are avoided. Unfortunately, many problems exist where it is impossible to tile the surface exactly using flat elements, especially when grid refinement is necessary near discontinuities, or when design features spoil the simple cylinder or sphere geometry. An example of this is a curved composite plate with a cutout, where the cutout plays the role of spoiler. If these plates have significant curvature, unacceptable inaccuracies could be expected.

Approximately a year ago, when the four and nine node assumed natural strain (ANS) elements were being developed [5], the often-used pinched hemisphere problem was chosen to check the elements out. Two grids were tried. The first was the usual polar grid with the single row of triangles near the apex, with the remainder as quadrilaterals exactly tiling the surface along latitude and longitude lines. The second was the grid shown in Figure 1, where a quarter of the sphere was modeled with symmetry along the sides and a free edge at the base. Note that this grid is in principle no worse than the first (in fact, the elements are well-formed, and no triangles are needed). To serve as a basis for comparison, the 410 element was run with both grids, again shown in Figure 1 (curves labeled *polar* for the polar grid, and *old* for the regular 410 in STAGS), where the ratio of displacement under the load to the converged solution is plotted as a function of the number of nodes along a side. Two things are striking about these results: (1) that the 410 element does so well with the polar grid, and (2) that it does so poorly with the seemingly harmless 'nonstandard' grid. This was all the more disappointing in view of the fact that for some coupled-field problems (such as in fluid-structure interaction applications), the latter grid is much preferred. One thing we noticed right away is that this problem is inextensional, an application where the linear bending theory in the 410 is well-suited. As these were all linear runs, it thus is not surprising that the 410 with the polar grid does well. Hence, the poor performance can be explained by studying the influence of the grid on the solution, and in particular, that the nodes cannot lie on the surface of the sphere and the elements at the same time. Apparently, equilibrium (determined at the *actual* node positions and calculated from a flat element) cannot be satisfied unless the much higher membrane stiffness comes into play. Thus the displacements are correspondingly reduced and the 410 misses the mark.

It was at this time that we realized that our corotational theory in principle *removes* most of the rigid-body motion before the elements use the displacements [7]. Could it be possible to solve this same problem for a very tiny load (assuring that real nonlinearity is absent) using a "nonlinear" algorithm with the corotation formulation? For the polar grid, the solution converged in one step with an absurdly tiny error to the same linear solution.

But for the other grid, convergence was difficult, with several step cuts. This solution is labeled *coro* in Figure 1, and it can be seen that the results were dramatically improved. No matter how small we made the load, the convergence was just as difficult, and the same solution (except for the load proportionality factor) came out. For this reason, we began to look at some of the details of the corotational implementation, to see if we had taken all factors into account, and to see if any effects of corotation could be extended to *linear* solutions. If it were possible to correct this deficiency in a manner largely external to the element, another "element-independent" method could be derived to extend and enhance existing inexpensive elements with relatively little effort. This is the subject of the next section.

2.1. The Corotational Theory: What's Missing?

It was apparent for some time that terms were missing in the previous formulation. To see this, we first summarize what steps must be undertaken when the element-independent [7] corotational procedure is used as part of a nonlinear iteration procedure:

Step 1) Prior to the calculation of stiffness or internal force, a new local element frame is calculated using the latest positions of the corner nodes. Given this new element frame and the latest orientations of the nodal surface triads, new deformational displacements are computed, including the element deformational *rotations*.

Step 2) Strains/stresses are calculated using the results of step 1), from which internal forces and (if needed) a new tangent stiffness are computed.

Step 3) New solution increments are obtained from the linearized problem in step 2), using standard matrix assembly and solution procedures. The unknowns are *incremental* displacements and rotations at the specified *nodes*.

Step 4) The solution increments are *composed* with the previous solution to produce a new solution. The composition law for the translations is the simple addition of the displacement increment with the proper value from the previous iteration. For rotations, a new *orthogonal rotation matrix* is first created, and the nodal triad is updated by the *product rule* for composing rotations.

In view of the behavior described in the previous section, we have concentrated on Step 2), that is, how a first and second variation of the strain energy is consistently derived *given* the element frame and deformational displacements from Step 1). All succeeding arguments assume that we are working within a single element, between a given iteration and a previous iteration. We have available to us the current solution, complete with deformational displacements and a new element frame. In addition, we know what the starting element coordinates, the starting element frame, and initial nodal surface triads were. Therefore, in what follows, we shall omit any reference to the assembly process and not worry about inter-element compatibility and assembly matters. The only reference to node number will be among those in a single element, a notation to be omitted when the meaning is obvious. Reference to the solution state will be with a single integer subscript in parenthesis, to be used only when necessary.

We now for the moment postulate that the local element strain energy is a scalar function of the local element deformational displacements only:

$$U = U(\mathbf{u}_e^{def}) \tag{2.1}$$

where U is the strain energy integrated over the element expressed as a function solely of quantities $\mathbf{u}_e^{def}$ defined at the *nodes*. For STAGS, this is at most a fourth-order polynomial in the displacement components. The relations

$$^a\mathbf{u}_e^{def} = \mathbf{E}_{(k)}^T(^a\mathbf{u}_g + ^aX_g - ^1\mathbf{u}_g) - X_e \tag{2.2}$$

and

$$^a\mathbf{D}_{(k)} = \mathbf{E}_{(k)}^T\,^a\mathbf{S}_{(k)}\mathbf{E}_{(0)} \tag{2.3}$$

define the deformational translations and rotations, respectively. Here, we are referring to state (k) at which a current solution is known, and to state (0) whose data we have saved for reference. The subscript g means that these quantities are in the *global* reference frame, and the subscript e refers to quantities defined in the *element* frame. X are *initial* nodal coordinates, defined relative to node 1 (see [7], where the corotational theory is developed in detail). The left superscript a refers to *node number*. There are in principle three translations and three rotations at each node a.

From Eq. (2.2) one can see that for the element frame defined in [7], there are exactly $6N-6$ independent translational quantities, where N is the number of nodes in the element. Since all distances are measured relative to node 1 (Eq. (2.2)), the three deformational translations are *zero* there. Similarly from the definition of the element frame in [7], it can be shown that the x in-plane displacement at node 4, and the lateral (w) displacement at node 3 are also zero. Finally, the lateral displacement at node 2 is *the same* as for node 4. Note that Eq. (2.2) is simply the statement that the local deformational displacement is the difference between the local element relative coordinates in deformed state k and the initial undeformed coordinates in the original element frame.

Eq. (2.3) is the analogue for rotations. $^a\mathbf{D}_{(k)}$ is the relative deformational rotation matrix needed to bring the nodal triad in line with the initial triad rotated *rigidly* with the local element frame.

The following definitions will explain the notation:

$\mathbf{E}_{(k)}$ — The local element frame for state k. Components originally defined in the *element* frame are transformed into the *global* frame. This is an orthogonal transformation. There is one and only one element frame per element per solution state k.

$^a\mathbf{S}_{(k)}$ — The amount required to rotate the initial nodal triad at node a from the initial state to the current state k. There are N such rotation matrices, one for each node a. One $^a\mathbf{S}(k)$ is attached to *each* node in the system, irrespective of the element connectivity. It is presumed to be uniquely defined and available for Step 2) above. This is also an orthogonal matrix.

${}^a\mathbf{D}_{(k)}$ The *relative* rotation required to bring the nodal triad (which rotates in response to the system demands, via the rotation composition law in Step 4)) in line with the same triad initially coincident but *rigidly* rotated with the element frame $\mathbf{E}_{(k)}$. This is a measure of local rotation that vanishes if the nodes and the element frame move as a unit. ${}^a\mathbf{D}_{(k)}$ is also an orthogonal matrix. Angular freedoms extracted from this triad [7] are used in the element strain computations.

$\mathbf{v}$ A bold lower-case Roman character refers to a vector quantity. It can be either an axial or a polar vector. When the distinction needs to be made, it will be explicitly pointed out. The dimensionality of the vector will depend on the context. Two exceptions to this notation are allowed: (1) the vector of *undeformed* relative nodal coordinates will be written as X (with appropriate subscripts), and the *deformed* relative nodal coordinates as x.

$[\mathbf{v}]$ A bold lower-case Roman character enclosed in a single set of brackets refers to a skew-symmetric *spin tensor* generated from a tree dimensional axial vector by the following correspondence principle:

$$[\mathbf{v}] = \begin{bmatrix} 0 & -v^3 & v^2 \\ v^3 & 0 & -v^1 \\ -v^2 & v^1 & 0 \end{bmatrix} \tag{2.4}$$

Here, the superscripts refer to *components*, not *powers*.

If the energy $U(\mathbf{u}_e^{def})$ is a unique differentiable function of the deformational displacements including rotations extracted from $\mathbf{D}_{(k)}$, then we can take its derivative. By the principal of virtual work, the first derivative of the strain energy with respect to the independent, admissible nodal *freedoms* will be the internal force. Unfortunately, the admissible nodal freedoms are not $\mathbf{u}_e^{def}$ and $\mathbf{D}$, but global total displacements and rotations. Without loss of generality, we take the translations as expressed in the global frame common to all elements (of course, if all freedoms at a given node are uniquely defined, any computational coordinate system would serve just as well). For rotations, we take the current orientation of the nodal triad as completely specifying nodal rotation data. This triad rotates *rigidly* with the node in response to the system, updated in Step 4) above. Thus we are faced with finding not only the explicit derivative of U, but also the derivative of the local displacements as a function of global quantities, as expressed in Eq. (2.2) and (2.3).

In the next section we shall examine the relation between the global and local displacements, and we shall reveal that for certain elements, terms presently omitted in the corotational theory can become important.

2.2. The Derivative of the Element Frame

We begin by taking the variation of Eq. (2.2):

$$\delta^a\mathbf{u}_e^{def} = (\delta\mathbf{E}_{(k)})^T({}^a\mathbf{u}_g + {}^aX_g - {}^1\mathbf{u}_g) + \mathbf{E}_{(k)}^T(\delta^a\mathbf{u}_g - \delta^1\mathbf{u}_g) \tag{2.5}$$

We take note that X_e and X_g are constant undeformed coordinates, and that all variations are functions solely of the global displacements. We make one important simplifying assumption at the outset: that all elements to be considered are invariant to arbitrary *translations*, something certainly true for the elements in STAGS. If that is the case, it is permissible to arbitrarily fix the displacement to zero at node 1 without changing the strain energy (in other words, there are at least three eigenmodes of the stiffness, linear or nonlinear, that are *rigid body translations* with zero eigenvalues). The second term in (2.5) is therefore simply the transformation from global coordinates to element coordinates, presently performed on both the stiffness and internal force before assembly. The *first term*, however, is not now included.

Before investigating this term, we take the variation of Eq. (2.3) to obtain

$$\delta^a \mathbf{D}_{(k)} = (\delta \mathbf{E}_{(k)})^T {}^a\mathbf{S}_{(k)} \mathbf{E}_{(0)} + \mathbf{E}_{(k)}^T \delta^a \mathbf{S}_{(k)} \mathbf{E}_{(0)} \tag{2.6}$$

Note that in both equations, we are faced with taking the variation of an orthogonal matrix. It is well known that for any orthogonal matrix $\mathbf{T}$,

$$\begin{aligned} [\delta\omega_T]_g \mathbf{T} &= \delta \mathbf{T} \\ [\delta\omega_T]_g &= (\delta \mathbf{T}) \mathbf{T}^T \end{aligned} \tag{2.7}$$

where $[\delta\omega_T]$ is a skew symmetric matrix representing the *infinitesimal rotations* of the base vectors of $\mathbf{T}$. Eq. (2.5) becomes

$$\delta^a \mathbf{u}_e^{def} = ([\delta\omega_E]_g \mathbf{E}_{(k)})^T ({}^a\mathbf{u}_g + {}^aX_g - {}^1\mathbf{u}_g) + \mathbf{E}^T (\delta^a \mathbf{u}_g - \delta^1 \mathbf{u}_g)$$

which reduces to

$$\delta^a \mathbf{u}^{def} = -\mathbf{E}_{(k)}^T [\delta\omega_E]_g {}^a x_g + \mathbf{E}^T \delta^a \mathbf{u}_g \tag{2.8}$$

where we have assumed that the ${}^1\mathbf{u}_g$ has been suppressed because the element is invariant to translations. Note that we have carried out the transpose and used the fact that the transpose of a skew-symmetric matrix is its negative. The quantity ${}^a x_g$ is the vector of *deformed* (undeformed plus displacements) coordinates of node a relative to node 1. Eq. (2.6) similarly becomes

$$\delta^a \mathbf{D}_{(k)} = -\mathbf{E}_{(k)})^T [\delta\omega_E]_g {}^a\mathbf{S}_{(k)} \mathbf{E}_{(0)} + \mathbf{E}_{(k)} [\delta^a\omega_S]_g {}^a\mathbf{S}_{(k)} \mathbf{E}_{(0)} \tag{2.9}$$

where similar operations to those in (2.8) were done here. Note that the skew-symmetric matrix $[\delta\omega_E]_g$ is a function of the current global nodal coordinates, dependent on the particular definition of the element frame in [7]. $[\delta^a\omega_S]_g$ is, on the other hand, an independent variation (in global coordinates) of the nodal triad at node a; these increments are the outcome of the solution process to be used in Step 4) above.

It proves more convenient to work in element coordinates, then transforming by standard procedures to the global frame after the local stiffness and internal force contributions have been calculated. The skew-symmetric tensor and its equivalent vector, *for orthogonal matrices only*, transform as follows:

$$\mathbf{r}_j = \mathbf{T}_{ji} \mathbf{r}_i; \qquad [\mathbf{r}]_j = \mathbf{T}_{ji} [\mathbf{r}]_i \mathbf{T}_{ji}^T \tag{2.10}$$

where j and i are two different coordinate systems. Using (2.10), Eqs. (2.8) and (2.9) can be expressed in local element coordinates as

$$\delta^a \mathbf{u}_e^{def} = -[\delta\omega_E]_e {}^a x_e + \delta^a \mathbf{u}_e \tag{2.11}$$

and

$$\delta^a \mathbf{D}_{(k)} = ([\delta^a \omega_S]_e - [\delta\omega_E]_e)^a \mathbf{D}_{(k)} \tag{2.12}$$

where it is understood that the components of the skew-symmetric tensors are relative to the element basis. ${}^a x_e$ and ${}^a \mathbf{u}_e$ are the relative deformed coordinates and displacements in the *element frame*. Alternate forms for Eq. (2.11) can be derived from the correspondence of the product of a skew-symmetric tensor with the cross product, specifically,

$$[\omega]\mathbf{r} = \omega \times \mathbf{r} = -\mathbf{r} \times \omega = -[\mathbf{r}]\omega \tag{2.13}$$

for any two three dimensional vectors $\mathbf{r}$ and ω. Eq. (2.11) can take either of the two forms

$$\begin{aligned} \delta^a \mathbf{u}^{def} &= -\delta\omega_E \times {}^a x_e + \delta^a \mathbf{u}_e \\ &= [{}^a x_e]\delta\omega_E + \delta^a \mathbf{u}_e \end{aligned} \tag{2.14}$$

where $\delta\omega_E$ is in *element coordinates* and where

$$[{}^a x_e] = \begin{bmatrix} 0 & -{}^a x_e^3 & {}^a x_e^2 \\ {}^a x_e^3 & 0 & -{}^a x_e^1 \\ -{}^a x_e^2 & {}^a x_e^1 & 0 \end{bmatrix}$$

is the spin tensor of the relative deformed coordinates for node a. Note that the spin tensor for node 1 vanishes since the coordinates are measured relative to that node. But Eq. (2.14) states that the variation in the deformational translations is modified only by an infinitesimal rotation of the element coordinates about node 1. Eq. (2.12), on the other hand, is already in the form used for the rotation composition law, something to be covered in much greater detail subsequently. (2.12) and (2.14) taken together state that the variation of the local deformational translations and rotations is modified by an infinitesimal rotation about node 1 with the axis of rotation in the direction of $\delta\omega_E$.

What does this mean physically? We return to the energy U and express its variation in terms of the global coordinates:

$$\delta U = \frac{\partial U}{\partial \bar{u}^j} \frac{\partial \bar{u}^j}{\partial u_g^i} \delta u_g^i = \bar{\mathbf{f}}^T \mathbf{J} \delta \mathbf{u}_g \tag{2.15}$$

where for clarity of notation we substitute $\bar{u}$ for u_e^{def}. Here, $\bar{\mathbf{f}}$ is the internal force vector corresponding to the deformational displacements, and $\mathbf{J}$ is the generalized Jacobian transformation from global to local coordinates embodied in Eqs. (2.12) and (2.14). The

new internal force, in terms of global coordinates (but expressed in components relative to the element frame) is

$$
\begin{aligned}
{}^{a}\mathbf{f}_{tr} &= {}^{a}\bar{\mathbf{f}}_{tr} + {}^{a}\bar{\mathbf{f}}_{tr}[{}^{a}x_e] \cdot \frac{d\omega_E}{d\mathbf{u}} = {}^{a}\bar{\mathbf{f}}_{tr} - {}^{a}x_e \times {}^{a}\bar{\mathbf{f}}_{tr} \cdot \frac{d\omega_E}{d\mathbf{u}} \\
{}^{a}\mathbf{f}_{r} &= {}^{a}\bar{\mathbf{f}}_{r} - {}^{a}\bar{\mathbf{f}}_{r} \cdot \frac{d\omega_E}{d\mathbf{u}}
\end{aligned}
\tag{2.16}
$$

where ${}^{a}\mathbf{f}_{tr}$ and ${}^{a}\mathbf{f}_{r}$ are the translational and rotational parts of the internal force, respectively. $d\omega_E/d\mathbf{u}$ is the yet undetermined variation of the spin tensor ω_E as a function of the displacements $\mathbf{u}$. Thus for each node in the system, the translational force is modified by the cross product of the current relative position coordinates of the node with the force, times the variation of the base vectors of $\mathbf{e}$ with respect to the displacements at all the nodes. Each of the moments is modified by the same derivative $d\omega_E/d\mathbf{u}$. Taken together, the internal forces are transformed by the quantity

$$\mathbf{P} = \mathbf{I} - \boldsymbol{\phi}\boldsymbol{\gamma}^T \tag{2.17}$$

through the relation

$$\mathbf{f} = \mathbf{P}^T\bar{\mathbf{f}} \tag{2.18}$$

where $\mathbf{I}$ denotes the identity matrix. Eq. (2.18) is fully equivalent to (2.16) when

$$\boldsymbol{\gamma}^T = \frac{d\omega_E}{d\mathbf{u}} \tag{2.19}$$

and

$$
\boldsymbol{\phi} = \begin{bmatrix}
 & \cdots & \\
0 & {}^{a}x^3 & -{}^{a}x^2 \\
-{}^{a}x^3 & 0 & {}^{a}x^1 \\
{}^{a}x^2 & -{}^{a}x^1 & 0 \\
 & & \\
 & \mathbf{I}_3 & \\
 & & \\
 & \cdots &
\end{bmatrix}
\tag{2.20}
$$

for a given node a. This relation is repeated for each node a, with the skew-symmetric portion belonging to the translations and the $3X3$ identity $\mathbf{I}_3$ to the rotations. $\boldsymbol{\phi}$ is a matrix containing a column of length six times the number of nodes N, or $6N$ for the general case of six freedoms per node. The first column corresponds to an infinitesimal

rotation about the x axis, the second about the y axis, and the third about the z direction in the local element frame. Each of these rotations in turn depends explicitly on the nodal positions at the corners. Close examination of the product $\phi^T \bar{\mathbf{f}}$ shows it to be equivalent to the relation

$$\sum_{a=1}^{N} ({}^a x \times {}^a\bar{\mathbf{f}}_{t_r} + {}^a\bar{\mathbf{f}}_r) \tag{2.21}$$

These are none other than the equations of moment equilibrium for the element, something that should be satisfied for all values of nodal displacements. It was one of the *fundamental assumptions* of the corotational theory that each element will be self-equilibrated with respect to the current configuration. Ideally, then, these new terms, with all the complications they bring, should vanish identically. The fact that they don't presents both an obstacle and an opportunity that have motivated the continuation of this research effort. The derivation of this matrix γ is the subject of the next section.

2.3. The Variation of the Element Frame

The infinitesimal rotation γ of the basis vectors of $\mathbf{E}$ (the *columns* of the transformation from the element local coordinates to global coordinates) is determined uniquely by the current nodal positions for both triangular and quadrilateral elements. There is one column of length $6N$ for each of the three directions, populated by the contributions from the motion of each of the corner nodes. For triangles, the element-local coordinate system has its origin at node 1, its y axis along the line joining nodes 1 and 3, and the z pointing out of the plane of the triangle. The x axis completes a right-hand system. For quadrilateral elements, the z axis is first defined as the cross product of the principal diagonals (lines joining nodes 1-3 and 2-4, respectively), the y is the *projection* of the 1-4 line on the plane with z as its normal and containing nodes 1 and 3, with the x axis completing a right-hand system. Details and pictures of these two cases are found in [7]. The total variation of the element frame with respect to the displacements is the product $\phi\gamma^T$. This is used in Eqs. (2.17) and (2.18) to calculate the internal force. In the two subsections that follow, γ will be derived for the special case of the triangle and quadrilateral elements, respectively.

2.3.1. Variation of the Element Frame—Triangles

For both triangles and quadrilateralss, only γ need be derived as a function of the infinitesimal local displacements, since the components are already in the element frame, and since transformation to any other frame requires only standard matrix operations using orthogonal matrices. Recall that the unit basis vector $\mathbf{e}_2$ of $\mathbf{E}$ lies in the direction of edge 1—3.

$$\mathbf{e}_2 = \frac{{}^3x}{|{}^3x|}. \tag{2.22}$$

For simplicity, we have omitted the reference to the element frame, as all quantities are defined in this frame. We recall also that these are the deformed coordinates for the

specified node, *relative to the origin at node 1*. $\mathbf{e}_3$ is defined as

$$\mathbf{e}_3 = \frac{{}^2x \times {}^3x}{D_3}, \tag{2.23}$$

D_3 is the magnitude of ${}^2x \times {}^3x$ needed to make $\mathbf{e}_3$ a unit vector. Its value is, specifically

$$D_3 = {}^2x \times {}^3x = {}^2x^1 \ {}^3x^2 \tag{2.24}$$

$|D_3|$ is equal to twice the area of the element. The right superscript refers to *components* along the local element basis vectors $\mathbf{e}_k$, $k = 1, 3$. The updated coordinates ${}^a x$ are related to the undeformed coordinates by the formula

$${}^a x = {}^a X + {}^a \mathbf{u} - {}^1 \mathbf{u} \tag{2.25}$$

where we must now include the displacement ${}^1\mathbf{u}$ at node one because its variation is permitted. We next vary each displacement in turn to see what change in each of the three basis vectors is generated, in effect generating the quantity $\delta \mathbf{e}_k$ directly. For example, from (2.22) and (2.25)

$$\delta \mathbf{e}_2 = \mathbf{e}_1(\delta^3 u^3 - \delta^1 u^3) + \mathbf{e}_3(\delta^3 u^1 - \delta^1 u^1) \tag{2.26}$$

Taking note that the relation between $[\delta \omega_E]_e$ and the variation of the element frame *in element coordinates* is (see Eqs. (2.7) and (2.10) and also Ref. [12])

$$[\delta \omega_E]_e = \mathbf{E}_{(i)}^T \delta \mathbf{E}_{(i)}$$

we have

$$\delta \omega_E^3 = -\mathbf{e}_1^T \delta \mathbf{e}_2 = \frac{\delta^1 u^1 - \delta^3 u^1}{{}^3x^2}$$

and

$$\delta \omega_E^1 = \mathbf{e}_3^T \delta \mathbf{e}_2 = \frac{\delta^3 u^3 - \delta^1 u^3}{{}^3x^2}$$

In these two equations, we note again that the displacement components have two superscripts: the left denotes the *node number* and the right the *component* number. For the base vectors $\mathbf{e}_k$, the subscript is the *base vector index* denoting the *direction* it points in the element system. Each column in $\mathbf{E}$ is one of those base vectors, and the components of these base vectors give the orientation of each of the three base vectors in the *global* system, since $\mathbf{E}$ is the transformation from element-local to global coordinates. The remainder of

the derivation is tedious but straightforward, yielding for γ the relation

$$\gamma = \begin{bmatrix} 0 & 0 & \frac{1}{3x^2} \\ 0 & 0 & 0 \\ -\frac{1}{3x^2} & \frac{1}{2x^1}\left(1 - \frac{2x^2}{3x^2}\right) & 0 \\ & \mathbf{0}_3 & \\ 0 & 0 & 0 \\ 0 & 0 & 0 \\ 0 & -\frac{1}{2x^1} & 0 \\ & \mathbf{0}_3 & \\ 0 & 0 & -\frac{1}{3x^2} \\ 0 & 0 & 0 \\ \frac{1}{3x^2} & \frac{2x^2}{2x^1 3x^2} & 0 \\ & \mathbf{0}_3 & \end{bmatrix} \tag{2.27}$$

where $\mathbf{0}_3$ is a three-by-three block of zeros corresponding to the rotational freedoms, verifying that γ is a function of the nodal *translations* only. Translational invariance is preserved even though it was not included in γ (we have assumed the elements are already invariant to translations): ***the column sums are identically zero***. That is, γ^T annihilates any pure translation. Note also that

$$\boldsymbol{\phi}^T\boldsymbol{\gamma} = \boldsymbol{\gamma}^T\boldsymbol{\phi} = \mathbf{I}_3 \tag{2.28}$$

a very important bi-orthogonality relation whose implications will be discussed later.

2.3.2. Variation of the Element Frame—Quadrilaterals

For quadrilaterals, we have from [7] the following:

$$\mathbf{e}_3 = \frac{{}^3\boldsymbol{x} \times ({}^4\boldsymbol{x} - {}^2\boldsymbol{x})}{D_3} \tag{2.29}$$

where

$$D_3 = {}^3x^1({}^4x^2 - {}^2x^2) - {}^3x^2({}^4x^1 - {}^2x^1)$$

is the normalizing factor. $|D_3|$ is equal to twice the area of the element projected on the plane defined by $\mathbf{e}_3$, nodes 1 and 3. We also have

$$\mathbf{e}_1 = \frac{{}^4x \times \mathbf{e}_3}{D_2}, \tag{2.30}$$

where

$$D_2 = {}^4x^2$$

The $\mathbf{e}_2$ axis required to complete a right-hand system is

$$\mathbf{e}_2 = \mathbf{e}_3 \times \mathbf{e}_1. \tag{2.31}$$

These manipulations are not unlike those for the triangles, yielding the following final results for γ:

$$\gamma_1 = \begin{bmatrix} 0 & 0 & \frac{1}{D_2} \\ 0 & 0 & 0 \\ \frac{{}^4x^1 - {}^2x^1}{D_3} & \frac{{}^4x^2 - {}^2x^2}{D_3} & \frac{{}^4x^3({}^4x^2 - {}^2x^2)}{D_2 D_3} \\ & \mathbf{0}_3 & \end{bmatrix} \tag{2.32}$$

$$\gamma_2 = \begin{bmatrix} 0 & 0 & 0 \\ 0 & 0 & 0 \\ -\frac{{}^3x^1}{D_3} & -\frac{{}^3x^2}{D_3} & -\frac{{}^4x^{33}x^2}{D_2 D_3} \\ & \mathbf{0}_3 & \end{bmatrix} \tag{2.33}$$

$$\gamma_3 = \begin{bmatrix} 0 & 0 & 0 \\ 0 & 0 & 0 \\ -\frac{{}^4x^1 - {}^2x^1}{D_3} & -\frac{{}^4x^2 - {}^2x^2}{D_3} & -\frac{{}^4x^3({}^4x^2 - {}^2x^2)}{D_2 D_3} \\ & \mathbf{0}_3 & \end{bmatrix} \tag{2.34}$$

$$\gamma_4 = \begin{bmatrix} 0 & 0 & -\frac{1}{D_2} \\ 0 & 0 & 0 \\ \frac{{}^3x^1}{D_3} & \frac{{}^3x^2}{D_3} & \frac{{}^4x^{33}x^2}{D_2 D_3} \\ & \mathbf{0}_3 & \end{bmatrix}. \tag{2.35}$$

where we have broken γ into contributions belonging to each of the four nodes. This quantity also applies to elements with more than 4 nodes, but the contributions belonging to any but the nodes that define the frame are identically zero. Again, γ does not spoil translational invariance, and the important bi-orthogonality relation (2.28) is obeyed (try that one out by direct substitution!).

2.3.3. Variation of the Element Frame—Beams

For beams, the definition of the element frame is more complicated. The x axis lies along the line joining the two beam nodes, and the z axis is the cross product of the y base vector ($\mathbf{q}_2$) of a triad rigidly attached to the surface triad ${}^1\mathbf{S}_{(k)}$ for node 1, but initially coincident with the *initial* element frame $\mathbf{E}_{(0)}$:

$$\mathbf{Q}_{(k)} = {}^1\mathbf{S}_{(k)}\mathbf{E}_{(0)} \tag{2.36}$$

where the initial element frame $\mathbf{E}_{(0)}$ is chosen in some unique way as function of translations only. See Ref. [7] for details. Using the same argument as for triangles and quadrilaterals, the following relations hold for the local rotations $\delta\boldsymbol{\omega}_E$:

$$\begin{aligned} \delta\omega_E^1 &= -\mathbf{e}_2^T\delta\mathbf{e}_3 \\ \delta\omega_E^2 &= -\mathbf{e}_3^T\delta\mathbf{e}_1 \\ \delta\omega_E^3 &= \mathbf{e}_2^T\delta\mathbf{e}_1 \end{aligned} \tag{2.37}$$

The variation of the base vector of the element frame $\mathbf{e}_1$ is a function only of displacements, and is derived in exactly the same way as with triangles. The result is

$$\begin{aligned} \delta\mathbf{e}_1 &= \frac{1}{l}[\mathbf{e}_2(\delta^2u^2 - \delta^1u^2) + \mathbf{e}_3(\delta^2u^3 - \delta^1u^3)] \\ l &= {}^2x^1 \end{aligned} \tag{2.38}$$

where $\mathbf{u}$ are displacements with components labeled by right superscripts and the node designation by left superscripts. l is the current length of the beam element, which by definition lies along the x axis. The variation of $\mathbf{e}_3$ is more complicated, but is straightforward, made much simpler by using the relation

$$\mathbf{e}_3^T\delta\mathbf{e}_3 = \mathbf{0}$$

After tedious calculations, the result is

$$\delta\mathbf{e}_3 = \frac{1}{q_2^2}\{\mathbf{e}_2[-\delta q_2^3 + \frac{q_2^1}{l}(\delta^2u^3 - \delta^1u^3)] - \frac{\mathbf{e}_1q_2^2}{l}(\delta^2u^3 - \delta^1u^3)\} \tag{2.39}$$

including all terms to first order. Note that all quantities are defined in the *element frame*, as was the case for triangles and quadrilaterals. The expression for $\delta\omega_E^3$ is derived by substituting (2.39) into (2.37) to yield

$$\delta\omega_E^3 = \frac{1}{q_2^2}[\delta q_2^3 - \frac{q_2^1}{l}(\delta^2u^3 - \delta^1u^3)] \tag{2.40}$$

$\delta\mathbf{Q}_e$ is related to the variation of the surface triad by the relation

$$\delta\mathbf{Q}_e = [\omega_S]_e\mathbf{Q}_e \tag{2.41}$$

where we have dropped the system state information and inserted the subscript e to emphasize the use of element coordinates. Combining (2.40), (2.41), (2.38), and using the same notation for γ as we had for triangles and quadrilaterals, we come up with the following final result:

$$\gamma = \begin{bmatrix} 0 & 0 & 0 \\ 0 & 0 & -\frac{1}{l} \\ \frac{\beta}{l} & \frac{1}{l} & 0 \\ 1 & 0 & 0 \\ -\beta & 0 & 0 \\ 0 & 0 & 0 \\ & \mathbf{0}_3 & \\ 0 & 0 & 0 \\ 0 & 0 & \frac{1}{l} \\ -\frac{\beta}{l} & -\frac{1}{l} & 0 \end{bmatrix} \tag{2.42}$$

where

$$\beta = \frac{q_2^3}{q_2^2}$$

Note that if for some reason the beam is so deformed that $\mathbf{q}_2$ lies along the x axis, our algorithm switches to the choice of the $\mathbf{q}_3$ as our $\mathbf{e}_3$ base vector, in which case everything here is derived as before except that β is set to zero. We leave that one as an exercise for the reader!

To calculate γ, we need $\mathbf{q}_2$ in *element coordinates*. To do this, we use the relation (2.10) (which applies to orthogonal matrices as well as spin tensors) and extract the second column:

$$\mathbf{q}_2 = \mathbf{E}_{(k)}^T {}^1\mathbf{S}_{(k)}\mathbf{E}_{(0)}\mathbf{e}_2 \tag{2.43}$$

It is gratifying that the bi-orthogonality relations still hold between ϕ and γ. The principal difference here is that the variation of the element frame is no longer independent of the rotations, with contributions dependent on the *variation of the surface triad*.

2.4. *The Projection Operator P*

Up to this point we have demonstrated that the matrix $\boldsymbol{\phi}$ represents an infinitesimal rotation about node 1 in three orthogonal directions corresponding to the base vectors of the element frame **E**. We have also shown that the inner product of $\boldsymbol{\phi}$ with the local internal forces reproduces the violation of rotational equilibrium in the three directions (Eq. 2.21). What remains is to show that the effect of infinitesimal rotations on the internal force modified by the product $\boldsymbol{\gamma}\boldsymbol{\phi}^T$ vanishes. If the element with modified internal forces is to satisfy equilibrium in the *updated* configuration, it must be invariant to *infinitesimal* rotations. Invariance to rotation is *completely equivalent* to the satisfaction of equilibrium, or the requirement that the element taken as a free body will be in rotational balance and will not move. What we must show is that

$$\boldsymbol{\phi}^T \mathbf{P}^T \bar{\mathbf{f}} = \mathbf{0} \tag{2.44}$$

where,

$$\mathbf{P} = \mathbf{I} - \boldsymbol{\phi}\boldsymbol{\gamma}^T$$

But given the bi-orthogonality relation (2.28), Eq. (2.44) holds. In fact, if a general displacement $\mathbf{d}$ is decomposed into

$$\mathbf{d} = \mathbf{d}_{def} + \boldsymbol{\phi}\boldsymbol{\alpha} \tag{2.45}$$

where $\mathbf{d}_{def}$ is the nonrotational part of the displacement, and $\boldsymbol{\alpha}$ is a vector of weighting coefficients for the rotational part of the displacement, we have

$$\begin{aligned} \mathbf{P}\mathbf{d} &= (\mathbf{I} - \boldsymbol{\phi}\boldsymbol{\gamma}^T)(\mathbf{d}_{def} + \boldsymbol{\phi}\boldsymbol{\alpha}) \\ &= \mathbf{d}_{def} + \boldsymbol{\phi}[\mathbf{I}_3 - (\boldsymbol{\gamma}^T\boldsymbol{\phi})]\boldsymbol{\alpha} - \boldsymbol{\phi}\boldsymbol{\gamma}^T\mathbf{d}_{def} \end{aligned} \tag{2.46}$$

The only way the contribution from the rigid-body part is always zero is if

$$\boldsymbol{\gamma}^T\boldsymbol{\phi} = \mathbf{I}_3$$

which is identical to the bi-orthogonality relation (2.28) that we have shown to hold for $\boldsymbol{\gamma}$ and $\boldsymbol{\phi}$. Thus the modified internal forces are strictly invariant to infinitesimal rotations (and translations for the elements in STAGS). In addition, if the element *nearly* obeys equilibrium in the first place, the quantity $\boldsymbol{\phi}^T\bar{\mathbf{f}}$ will be small, and the internal force and stiffness for the deformational part of the displacements will be only slightly altered. This translates into improved performance for the warping problem, because it is the rotations about an axis perpendicular to the element plane, which can be much larger than deformational displacements across the area of the element, that spoils performance. In a sense, this is the analogue of the corotational theory in the *linear* limit, because if local equilibrium fails in that limit, the influence of **P** does not vanish.

Before reviewing the effect that **P** has had on various elements, we first mention that **P** is a *projection operator*. Projection operators have no inverse (this **P** is of rank $N-3$), and satisfy the relation

$$\mathbf{P}^2 = \mathbf{P}$$

Projection operators are annihilators: they project out or reduce the vector space, in this case, removing the three rigid rotations. What is powerful about this particular projection operator is that it was consistently derived from the corotational theory that has already proven itself. The vectors ϕ and γ are well conditioned (unless the area of the element is zero) and dimensionally consistent, with the translational parts of ϕ having the units of length, and γ its natural inverse with units of one over length. No arbitrary orthogonalization was necessary, as orthogonality just "fell out" as a result of taking consistent derivatives. This suggests that the method will be applicable no matter what element frame is chosen, such as the more complicated element frame for beams [7].

Finally, we mention that while the internal force is modified by the relation in Eq. (2.18), the linear stiffness is modified by the usual equivalence transformation

$$\mathbf{K} = \mathbf{P}^T \bar{\mathbf{K}} \mathbf{P} \tag{2.47}$$

The derivation of (2.47) is straightforward, and its implementation follows standard procedures already in place.

2.5. Element Performance—Results

In the beginning, the projector was added to the 410 element and tested with planar and cylinder configurations that do not have warping. No difference whatever was seen between the old and new 410 for *linear* analyses, indicating that the 410 obeys equilibrium in the linear limit regardless of element distortions within a plane. The result reinforces the belief that, for a majority of cases, the current implementation of the 410 suffices.

Figure 1 shows what happens when the SH410 element is run with the projection $\mathbf{P}$ in place (linear analysis) for a case where warping *does* exist. Note the improved performance of the 410 even over the nonlinear results discussed earlier. As expected, this time when the projection operator was included, the nonlinear solution required only a single iteration (with an absurdly small error) that reproduced the linear solution almost exactly, even at the unit loads used in this analysis.

Figures 2 and 3 summarize the effect of $\mathbf{P}$ on various elements. Included are the STAGS 410, the four node ANS [6] (4_ANS), an experimental hybrid element [4] (HYB), and the nine node ANS curved element [5] shown for reference (it is curved and is insensitive to warping). Fig. 2 is the same pinched hemisphere problem as for Fig. 1. The 4_ANS is K. C. Park's element that has been shown to be sensitive to warping. Clearly the projector improves performance significantly. Even the HYB element is helped, which means local equilibrium is not truly satisfied.

Fig. 3 is the pinched cylinder problem presented in [10], where this time distortion angle is the parameter. The grids chosen were different for each of the elements, so that for zero distortion, one begins with a *converged* solution. The sensitivity to distortion (a typical grid shown in the figure) is measured by computing the solution as a function of the orientation of the central element (see figure). At about 40°, the area of the adjacent elements is nearly zero, presenting a "worst case". Warping is important in this problem because when the grid lines no longer follow the generators of the cylinder, the element

nodes cannot both lie on the cylinder and on the flat element segments. The results for this problem are just as dramatic as for the pinched hemisphere. All flat elements are improved, with the STAGS 410 element one of the best performers. What a contrast to the unaltered case! The old 410 essentially locked and was completely useless for even the most modest distortion angles. We want to mention that for the case of $r/h = 50$, *all* elements reproduced the converged solution no matter what the distortion. These results are not shown here. For a look at how they performed before projection see [10].

3. The Problem of Slow Convergence

Soon after the corotational theory was implemented in STAGS, we recognized that convergence to *nonlinear* solution states had deteriorated somewhat, depending on the nature of the case investigated. True Newton cases no longer acted like true Newton, in that the quadratic, or superlinear convergence was lost. Clearly the second variation was not completely consistent with the first variation of the strain energy; this problem appeared whenever corotation was turned on, regardless of the type of analysis, and regardless of whether the external loads were conservative or not. A clue that some degree of incompatibility that might exist in the tangent stiffness was clear even for the Mak arch [3] chosen in [7] as a benchmark for the corotational implementation. For the SH410 element, the sign of the determinant of the tangent stiffness did not change at the instant the load crossed the limit point, as of course it must. An associated problem was the sensitivity of the corotational analysis to the frequency of element frame updates. The solution came out differently when the frame was updated *every iteration* as opposed to *each converged load step* as was originally proposed in [7]. This was disturbing because the 41X family of elements was advertized and tested for *moderate* rotations at least up to 10 or 15°. Ideally, one should be able to "turn off" corotation for a while, do some load steps in the neighborhood of a converged state using as a base the element frame calculated there, and then repeat the process. One could realize possible improvements in efficiency, and certainly have better confidence in the method if the answers were not sensitive to such choices. The fact that, as corotation is now configured, the answers *are* sensitive to the frequency the element frame updates has been part of the reason for conducting the research that has led to the results to be covered in this section.

Section 3 is divided into three main subsections as follows:

1) In the first subsection, we shall demonstrate nonsymmetry in a *numerically-calculated* tangent stiffness (using only first variations), even for a supposedly *converged* equilibrium state. We shall discuss what consequences this nonsymmetry has on both the underlying assumptions of the corotational theory and solutions calculated using the theory.

2) In the second subsection, we shall introduce three simple sample problems to explain what is going on. Each problem has an analogue in the real finite element world, and together they cover the features we are interested in, including the nonsymmetry questions in 1).

3) In the last subsection, the effect of the *second derivative* of the relations (2.2) and (2.3) that define the transformation from the global, total displacements to the local, deformational displacements will be discussed. A way to account for the greater contribution of these derivatives based solely on global invariance properties will be derived.

By combining the what is learned from these three areas, we will demonstrate the recovery of true Newton convergence for a real STAGS 410 analysis for a problem with conservative loads.

3.1. *The Nonsymmetric Tangent Stiffness*

After we had derived and implemented the projection operator **P** for the SH410 element, the next question was what would be the effect on a *nonlinear* analysis. We first altered the *material* (as opposed to geometric) stiffness by the relation in Eq. (2.47), and tried this on some sample test cases. We were gratified that the results did not change much, except that convergence was no better than without **P**. We discovered that **P** *did*, in fact, modify the nonlinear results slightly even for planar problems, indicating that the geometrically nonlinear element no longer obeys equilibrium relative to the *deformed state*.

The next logical step was to get a closer look at the tangent stiffness for the element in some nonlinear configuration that contained nontrivial rotations. One excellent means of doing this is to do as many first variations as there are freedoms, perturbing each freedom in turn by a "tiny" amount, and taking the ratio of the difference from some reference state to the increment chosen. As this is the *definition* of the partial derivative, it should converge for some value of the increment. It is to be noted that by perturbation, we mean traversing all the steps in the corotational theory from Step 1) through 4), omitting only 3) because the increment is a given and not solved for. This means that when a rotational freedom is incremented by a small amount, a full rotation matrix *corresponding* to this increment is created and *composed* with the previous nodal triad to produce a new one. Rotations are combined by the *product rule* as follows:

$$ {}^{a}\mathbf{S}_{(k+1)} = \Delta^{a}\mathbf{S}_{(k+1,k)}\,{}^{a}\mathbf{S}_{(k)} \tag{3.1} $$

where we are using the proper notation for the *nodal surface triad*. The quantity $\Delta^{a}\mathbf{S}_{(k+1,k)}$ is the rotation matrix, presumably very close to the identity, derived from the perturbation of a given rotational freedom. This rule is in contrast to the ordinary *addition rule* used for translational freedoms.

When this process is carried out (including the calculation of new element frames, etc.) the resulting stiffness turns out to be nonsymmetric and different in many respects from that calculated by standard means. This poses a problem, because it is well known that for a conservative system loaded only by point forces in a fixed direction, the stiffness matrix *must* be symmetric if the linearization is carried out consistently. At this point we decided to backtrack to some simple problems that embodied Steps 1) through 4) in the full corotational theory, but at the same time could be fully understood.

3.2. *Sample Problems—Introduction*

We will begin with a problem defined by unit position vectors only, a problem whose linearization is straightforward, easily understood, and important in its own right. We shall follow this with a problem that is instead a function of a pseudovector (angles), and show what has to happen when the product rule is used to update the system state. Finally, we shall investigate what difference the choice of the pseudovector makes (if any), and what this means for a finite element analysis. The third and the second problem will be the same except for the normalization of the pseudovector.

3.2.1. The Function of a Unit Vector

Our first sample problem has a potential that depends on *unit* vectors only, including the external force. This problem belongs to a general class of potential functions where rotations are replaced by *shell normals* at the nodes, so that exactly 2 rotational freedoms exist per site. Most C^0 shell elements belong to this class, where there are *five* freedoms per node, with three translational freedoms and two rotations. Potentials defined by these normal vectors are well-defined, conservative, and very straightforward to linearize.

3.2.1.1. The Definition of the Potential U

The sample potential chosen is

$$U(\hat{\mathbf{r}}_1, \hat{\mathbf{r}}_2, \hat{\mathbf{r}}_3) = \frac{1}{2}(k_1\epsilon_1^2 + k_2\epsilon_2^2 + k_{12}\epsilon_{12}^2) + \frac{1}{2}\sum_{i=1}^{3} m_i(\hat{r}_{i+2}^i - \hat{r}_i^{i+2}) \tag{3.2}$$

where the index i is counted cyclicly from 1 to 3. For example, if $i = 2$, then $i+1 = 3$ and $i+2 = 1$. The subscripts label three mutually perpendicular vectors $\hat{\mathbf{r}}_i$ that rotate rigidly as a group. The roman superscripts denote *components* of $\hat{\mathbf{r}}$. The ϵ's are "strains" defined by

$$\begin{aligned} \epsilon_1 &= \hat{r}_1^3 = \mathbf{e}_3 \cdot \hat{\mathbf{r}}_1 \\ \epsilon_2 &= \hat{r}_2^3 \\ \epsilon_3 &= \frac{1}{2}(\hat{r}_1^2 - \hat{r}_2^1) \end{aligned} \tag{3.3}$$

where we have introduced the notation $\mathbf{e}_k$ to denote the base vector in the fixed coordinate system. This problem is like a little "beam" segment tied to springs (Fig. 4). The first three terms in U simulate the bending energy of the segment. The second part of the potential defined by the sum simulates *external moments* to which they reduce for small angles. k and m are constants that define the magnitudes of the "internal energy" and "external forces," respectively.

3.2.1.2. The Linearization of the Potential

Eqs. (3.2) and (3.3) constitute a conservative, nonsingular system with *three* freedoms, that is, the three quantities that define the *rotation operator* that brings this rigid triad $\{\hat{\mathbf{r}}_1, \hat{\mathbf{r}}_2, \hat{\mathbf{r}}_3\}$ in into a position of minimum energy. These three freedoms are defined *implicitly* through the nodal triad, just as in STAGS and other structural analysis codes. There is no ambiguity if we begin by selecting some *initial position* for triad $\mathbf{r}_1, \mathbf{r}_2, \mathbf{r}_3$, and by selecting the *identity* as the initial rotation operator. After the initial state is specified, we simulate Steps 1) through 4) (Section 2). During this entire sequence, the freedoms appear *explicitly* only as *increments* during the solution and update stages (Steps 3) and 4)).

Steps 1) and 4) can be combined after the initial iteration because after the update, we have available the "local" rotations from the triad $\{\hat{\mathbf{r}}_1, \hat{\mathbf{r}}_2, \hat{\mathbf{r}}_3\}$ that completely determines

the energy and its derivatives. For Step 2), we must linearize the energy with respect to *infinitesimal* rotation increments. Fortunately, for vectors, we know the relation between an infinitesimal rotation and the variation of the vector:

$$\delta\hat{\mathbf{r}}_k = \delta\boldsymbol{\omega} \times \hat{\mathbf{r}}_k \tag{3.4}$$

for any small rotation $\delta\boldsymbol{\omega}$. In what follows, we will need to use the relations

$$\begin{aligned} \mathbf{u}\cdot\mathbf{v}\times\mathbf{w} &= \mathbf{u}\times\mathbf{v}\cdot\mathbf{w} \\ \mathbf{u}\times(\mathbf{v}\times\mathbf{w}) &= \mathbf{v}(\mathbf{u}\cdot\mathbf{w}) - \mathbf{w}(\mathbf{u}\cdot\mathbf{v}) \\ \mathbf{u}\times\mathbf{v} &= -\mathbf{v}\times\mathbf{u} \end{aligned} \tag{3.5}$$

from vector analysis. Using (3.4) and (3.5) and the notation $\mathbf{e}_k$ to denote unit fixed base vectors in the global system, we have

$$\begin{aligned} \delta U = [&k_1\epsilon_1\hat{\mathbf{r}}_1\times\mathbf{e}_3 + k_2\epsilon_2\hat{\mathbf{r}}_2\times\mathbf{e}_3 + \frac{k_{12}\epsilon_{12}}{2}(\hat{\mathbf{r}}_1\times\mathbf{e}_2 - \hat{\mathbf{r}}_2\times\mathbf{e}_1) \\ &\frac{1}{2}\sum_{i=1}^{3} m_i(\hat{\mathbf{r}}_{i+2}\times\mathbf{e}_{i+1} - \hat{\mathbf{r}}_{i+1}\times\mathbf{e}_{i+2})]\cdot\delta\boldsymbol{\omega} \end{aligned} \tag{3.6}$$

where the same cyclic summation over indices is used.

The second derivative is straightforward, but tedious, with liberal use of relations (3.5). This tangent stiffness separates naturally into two parts, the first being a "*material*" stiffness wherein the variation takes place again as a function of the unit vectors, to be then expressed as a function of the incremental rotations $\delta\boldsymbol{\omega}$. Specifically,

$$\delta^2 U = \delta\hat{\mathbf{r}}_i^T \frac{\partial^2 U}{\partial\hat{\mathbf{r}}_i\partial\hat{\mathbf{r}}_j}\delta\hat{\mathbf{r}}_j + \delta^2\mathbf{r}_j\left(\frac{\partial U}{\partial\mathbf{r}_i}\right) \tag{3.7}$$

where the first term is the "material" stiffness. The second term is a "*geometric*" part, defined by the *second variation* of the unit vectors $\hat{\mathbf{r}}_k$ as a function of the incremental rotations. The material stiffness is

$$\begin{aligned} \mathbf{K}_{mat} = &k_1(\hat{\mathbf{r}}_1\times\mathbf{e}_3)(\hat{\mathbf{r}}_1\times\mathbf{e}_3)^T + k_2(\hat{\mathbf{r}}_2\times\mathbf{e}_3)(\hat{\mathbf{r}}_2\times\mathbf{e}_3)^T \\ &+ \frac{1}{4}(k_{12}(\hat{\mathbf{r}}_1\times\mathbf{e}_2 - \hat{\mathbf{r}}_2\times\mathbf{e}_1)(\hat{\mathbf{r}}_1\times\mathbf{e}_2 - \hat{\mathbf{r}}_2\times\mathbf{e}_1)^T \end{aligned} \tag{3.8}$$

Note that the "external loads" do not appear in the "material" stiffness, and that the material stiffness is strictly symmetric, regardless of the state of the system, equilibrium or not. The "geometric" stiffness is

$$\begin{aligned} \mathbf{K}_{geom} = &\frac{1}{2}\sum_{i=1}^{3} m_i[\hat{\mathbf{r}}_{i+2}\mathbf{e}_{i+1}^T - \mathbf{e}_{i+1}\mathbf{e}_{i+2}^T + \mathbf{I}(\hat{\mathbf{r}}_{i+1}\cdot\mathbf{e}_{i+2} - \hat{\mathbf{r}}_{i+2}\mathbf{e}_{i+1})] \\ &+ k_1\epsilon_1(\hat{\mathbf{r}}_1\mathbf{e}_3^T - \mathbf{I}\hat{\mathbf{r}}_1\cdot\mathbf{e}_3) + k_2\epsilon_2(\hat{\mathbf{r}}_2\mathbf{e}_3^T - \mathbf{I}\hat{\mathbf{r}}_2\cdot\mathbf{e}_3) \\ &+ \frac{k_{12}\epsilon_{12}}{2}[\hat{\mathbf{r}}_1\mathbf{e}_2^T - \hat{\mathbf{r}}\mathbf{e}_1^T + \mathbf{I}(\hat{\mathbf{r}}_2\cdot\mathbf{e}_1 - \hat{\mathbf{r}}_1\cdot\mathbf{e}_2)] \end{aligned} \tag{3.9}$$

where cyclic index notation applies, and where we have kept the inner products $\hat{\mathbf{r}}_k \mathbf{e}_j = \hat{r}_k^j$ to emphasize the *structure* of the geometric stiffness $\mathbf{K}_{geom}$.

The most obvious property of the geometric stiffness is that it is, in general, *nonsymmetric*. However, it can be shown by direct substitution that if (3.6) holds, the stiffness is *always* symmetric. That is, for any *equilibrium* configuration, the stiffness must be symmetric for conservative systems. Note that by conservative, we mean definable by a potential. The first and second variations of the "external" loads must also be consistently derived, which of course includes the contribution of the so-called "load stiffness" to Eq. (3.9). The second obvious property is the repetition of the sequence

$$\hat{\mathbf{r}}_k \mathbf{e}_j^T - \mathbf{I}\hat{\mathbf{r}}_k \cdot \mathbf{e}_j \tag{3.10}$$

for various indices k and j. It turns out that there is a *generalization* of (3.8) and (3.9) that makes use of this pattern. We shall show this subsequently.

3.2.1.3. The Solution of the First Sample Problem

Small, in-core utilities that simulate Steps 2), 3) and 4) were put together into a true Newton-Raphson solver to be used for arbitrary combinations of the constants k_i and m_i, and arbitrary starting configurations of the triad $\{\hat{\mathbf{r}}_1, \hat{\mathbf{r}}_2, \hat{\mathbf{r}}_3\}$. The surface triad update routine from the STAGS corotational software (Subroutine UPSTR) was altered to create a rotation operator from the relation

$$\mathbf{S}(\omega_S) = \exp([\omega_S]) \tag{3.11}$$

This is the general relation connecting *any* skew-symmetric matrix $[\omega_S]$ to the rotation operator $\mathbf{S}$. Eq. (3.11) has been discussed at length by ARGYRIS [2], SIMO [8,9] and many others. The modifications to UPSTR are minor, involving only the renormalization of the pseudovector defined in [7] to conform to (3.11). In all other respects, the solution sequence was just like any ordinary Newton-Raphson iteration loop, with the definition of the internal force by Eq. (3.6), and the tangent stiffness by sum of $\mathbf{K}_{mat}$ and $\mathbf{K}_{geom}$ (Eqs. (3.8) and (3.9)). A new factorization was carried out for each iteration, solution increments were solved for, and Eq. (3.11) was invoked to create an incremental rotation. This incremental rotation was applied to the latest configuration of the triad $\{\hat{\mathbf{r}}_1, \hat{\mathbf{r}}_2, \hat{\mathbf{r}}_3\}$ to create the next configuration. The error norm of the residual (Eq. (3.6)) was then calculated for output. This cycle was repeated as many times as desired, and the convergence was manually monitored as the solution progressed. We have included the option to leave the stiffness alone, or to symmetrize it before factorization was put in place to see what effect this would have on convergence.

The first runs were made using the ordinary, nonsymmetric stiffness. As many arbitrary combinations of the input were tried as time permitted, with the outcome *always exactly the same*: after a few starting iterations (that number depended somewhat on the initial conditions), the error diminished *at least quadratically* like true Newton should, with the error norm at step i being roughly the *square* of the previous norm. This behavior shows that the linearization in Eqs. (3.6) through (3.9) is completely consistent with the

update formula (3.11), and that (3.4) indeed defines properly the variation of a unit vector in three-dimensional space. The next runs were identical, except that the stiffness was *symmetrized* first. The outcome to this set of runs was almost identical! It was even the same when the *transpose* of the stiffness was used, implying that *any* scalar times the skew-symmetric part of the stiffness could be added to the symmetrized stiffness without substantial change to the solution convergence. Bahram Nour-Omid has explained this behavior with a very simple proof, shown in the next section.

3.2.1.4. Convergence with the Symmetrized Stiffness

Consider the semi-Newton algorithm given as follows for the solution of the equation

$$\mathbf{f}(\mathbf{x}) = \mathbf{0} \tag{3.12}$$

where $\mathbf{f}$ is a vector function of vector $\mathbf{x}$.

Given an initial guess $\mathbf{x}(i)$:

$$\begin{aligned} &1) && \mathbf{K}_{(i)} = \left.\frac{\partial \mathbf{f}}{\partial \mathbf{x}}\right|_{\mathbf{x}=\mathbf{x}_{(i)}} \\ &2) \quad \text{Solve} && \mathbf{K}^s_{(i)} \Delta \mathbf{x}_{(i)} = -\mathbf{f}(\mathbf{x}_{(i)}) \\ &3) && \mathbf{x}_{(i+1)} = \mathbf{x}_{(i)} + \Delta \mathbf{x}_{(i)} \end{aligned} \tag{3.13}$$

where we define the quantities

$$\begin{aligned} \mathbf{K}^s &= \frac{1}{2}(\mathbf{K} + \mathbf{K}^T) \\ \mathbf{K}^a &= \frac{1}{2}(\mathbf{K} - \mathbf{K}^T) \end{aligned} \tag{3.14}$$

Theorem

The rate of convergence of the above algorithm defined by steps 1) through 3) in (3.13) as constituting an iteration cycle is quadratic if

$$||\mathbf{K}^a_{(i)}|| \leq \alpha ||\mathbf{f}(\mathbf{x}_{(i)})|| \tag{3.15}$$

where α is a constant.

Proof

The Taylor series expansion at $\mathbf{x}_{(i)}$ is

$$\mathbf{f}(\mathbf{x}_{(i)}) = \mathbf{f}(\mathbf{x}_{(i-1)}) + \mathbf{K}_{(i-1)} \Delta \mathbf{x}_{(i-1)} + \mathbf{r}(\Delta \mathbf{x}_{(i-1)}) \tag{3.16}$$

where $\mathbf{r}$ is the remainder which depends on $\Delta \mathbf{X}_{(i-1)}$ and

$$||\mathbf{r}(\Delta \mathbf{x}_{(i-1)})|| \leq \beta ||\Delta \mathbf{x}_{(i-1)}||^2 \tag{3.17}$$

with β some other constant. Writing $\mathbf{K}_{(i-1)}$ in terms of its symmetric and skew-symmetric parts, we have

$$\mathbf{f}(\mathbf{x}_{(i)}) = \mathbf{f}(\mathbf{x}_{(i-1)}) + \mathbf{K}^s_{(i-1)}\Delta\mathbf{x}_{(i-1)} + \mathbf{K}^a_{(i-1)}\Delta\mathbf{x}_{(i-1)} + \mathbf{r}(\Delta\mathbf{x}_{(i-1)})$$

By using the second of Eq. (3.13) for the $i-1$'st iteration, we have

$$\mathbf{f}(\mathbf{x}_{(i)}) = \mathbf{K}^a_{(i-1)}\Delta\mathbf{x}_{(i-1)} + \mathbf{r}(\Delta\mathbf{x}_{(i-1)}) \tag{3.18}$$

Then,

$$\Delta\mathbf{x}_{(i)} = -(\mathbf{K}^s_{(i)})^{-1}\{\mathbf{K}^a_{(i-1)}\Delta\mathbf{x}_{(i-1)} + \mathbf{r}(\Delta\mathbf{x}_{(i-1)})\} \tag{3.19}$$

and taking norms

$$||\Delta\mathbf{x}_{(i)}|| \leq ||(\mathbf{K}^s_{(i)})^{-1}||\{||\mathbf{K}^a_{(i-1)}||\ ||\Delta\mathbf{x}_{(i-1)}|| + ||\mathbf{r}(\Delta\mathbf{x}_{(i-1)})||\} \tag{3.20}$$

But

$$||\mathbf{K}^a_{(i-1)}|| \leq \alpha||\mathbf{f}(\mathbf{x}_{(i-1)}|| \leq \alpha||(\mathbf{K}^s_{(i-1)}||\ ||\Delta\mathbf{x}_{(i-1)}|| \tag{3.21}$$

Then,

$$||\Delta\mathbf{x}_{(i)}|| \leq ||(\mathbf{K}^s_{(i)})^{-1}||\{\alpha||(\mathbf{K}^s_{(i-1)})^{-1}||\ ||\Delta\mathbf{x}_{(i-1)}||^2 + \beta||\Delta\mathbf{x}_{(i-1)}||^2\} \tag{3.22}$$

or

$$||\mathbf{x}_{(i+1)} - \mathbf{x}_{(i)}|| \leq \gamma_i||\mathbf{x}_{(i)} - \mathbf{x}_{(i-1)}||^2 \tag{3.23}$$

where

$$\gamma_i = ||(\mathbf{K}^s)^{-1}||(\alpha||(\mathbf{K}^s_{(i-1)})^{-1}|| + \beta) \tag{3.24}$$

Q.E.D

Thus if the antisymmetric part of the stiffness vanishes as the same rate as the residual, convergence is quadratic whether the symmetrized or unsymmetrized stiffness is used. But this is just our situation: the nonsymmetric part of the stiffness is proportional to the residual, something to be proved for the *general* function of a unit vector, in the next section.

3.2.1.5. The General Function of the Unit Vector

We now generalize what we have found for the special, but reasonable potential defined by (3.2). Take *any* function of a *set* of unit vectors ${}^a\hat{\mathbf{r}}$, and for the time being assume that each is *independent* of the other (two independent freedoms defined per vector):

$$U = U({}^1\hat{\mathbf{r}}, {}^2\hat{\mathbf{r}}, \cdots, {}^N\hat{\mathbf{r}}) \tag{3.25}$$

defining some twice-differentiable function U as a *scalar* dependent only on the *components* of the ${}^a\hat{\mathbf{r}}$ for "nodes" $a = 1, N$. The first variation, using (3.4) and relations (3.5), for *each* "*node*" a is the following:

$${}^a\mathbf{f} \cdot \delta^a\boldsymbol{\omega} = {}^a\hat{\mathbf{r}} \times {}^a\bar{\mathbf{f}} \cdot \delta^a\boldsymbol{\omega} \tag{3.26}$$

where

$$ {}^a\bar{\mathbf{f}} = \frac{\partial U}{\partial {}^a\hat{\mathbf{r}}} \tag{3.27} $$

is a vector of length three belonging to "node" a. Eq. (3.26) has an obvious interpretation: ${}^a\mathbf{f}$ is the "moment" constructed from the cross product of the unit vector with the "force" ${}^a\bar{\mathbf{f}}$ at its tip. The condition of equilibrium is for these internal moments to balance any external moments. The residual from an assemblage of moments so calculated must also vanish. The problem defined by (3.2) is such an assemblage. We in that case had *three* vectors driven by a *single* rotation. The first variation of (3.2) could have been derived by first taking the derivative with respect to the *components* of the three vectors as if they were independent quantities, then using (3.26) to relate them to three *separate* rotations. Since these three rotations are actually *the same*, the parts belonging to a given component of these rotations are *added*, yielding the same results as those computed directly (Eqs. (3.6), (3.7) and (3.9)) for the first and second variations. Of course this step is completely analogous to the *assembly* step in finite element analysis (part of Step 3), Section 2).

For the second variation, it is straightforward to derive the following:

$$ \mathbf{K}_{mat} = \mathbf{Z}^T \bar{\mathbf{K}} \mathbf{Z} \tag{3.28} $$

where $\mathbf{Z}$ is block diagonal, with exactly N blocks, or one for each independent rotation. Each block contains skew-symmetric 3 x 3 matrix

$$ {}^a\mathbf{Z} = -[{}^a\hat{\mathbf{r}}] \tag{3.29} $$

The second part of the stiffness is

$$ {}^a\mathbf{K}_{geom} = {}^a\hat{\mathbf{r}}\, {}^a\bar{\mathbf{f}}^T - \mathbf{I}_3({}^a\hat{\mathbf{r}} \cdot {}^a\bar{\mathbf{f}}) \tag{3.30} $$

Note the similarity of (3.30) to (3.10); the fact that (3.9) is a special case of (3.30) shows clearly as a repetition of the structure in (3.30), with N of these ${}^a\mathbf{K}_{geom}$ blocks placed along the diagonal. (3.28) and (3.29) are derived by considering a single-node system and generalizing. The total stiffness is the sum of the "material" and "geometric" contributions. In (3.28), $\bar{\mathbf{K}}$ is the second variation of the potential with respect to the *components* of the unit vectors, or

$$ \bar{\mathbf{K}} = \frac{\partial^2 U}{\partial {}^a\mathbf{r} \partial {}^b\mathbf{r}} \tag{3.31} $$

The matrix in (3.31) could, in principle, be full.

Some general comments are in order. First, each submatrix is of rank 2. This is true because

$$ [{}^a\mathbf{r}]{}^a\mathbf{r} = {}^a\mathbf{r} \times {}^a\mathbf{r} = \mathbf{0} \tag{3.32} $$

and because

$$ {}^a\mathbf{K}_{geom}\, {}^a\mathbf{r} = \mathbf{0} \tag{3.33} $$

Thus, a set of rotations each in the direction of its unit vectors cannot change their position, hence cannot change the energy or internal force.

Second, the tangent stiffness, is, in general, nonsymmetric. However, when the moments are zero, then

$$ {}^a\mathbf{r} \times {}^a\bar{\mathbf{f}} = \mathbf{0} $$

so that

$$ {}^a\bar{\mathbf{f}} = c\,{}^a\mathbf{r} $$

where c is some constant. Clearly then the stiffness is symmetric, confirming the proposition that the stiffness *must* be symmetric whenever a conservative system is in equilibrium. Direct calculation of the off-diagonal skew-symmetric portion of the geometric stiffness confirms that skew-symmetric portion of the stiffness vanishes according to the following general relation

$$ {}^a\mathbf{K}^a_{geom} = \frac{1}{2}[{}^a\mathbf{f}] \tag{3.34} $$

something proved by ARGYRIS in [1] for the general case. Hence, for *any* system that is a function of unit vectors, we can use (3.26) for the first variation, (3.28) and the symmetrized version of (3.30) to complete the linearization with the second variation.

For those functions that depend *also* on position vectors, we can easily generalize what we have. The first variation for the translational part does not require the modifications derived here; for the rotational part, the internal force is modified by the relation

$$ {}^a\mathbf{f} = {}^a\hat{\mathbf{r}} \times {}^a\bar{\mathbf{f}} \tag{3.26} $$

for each node a. For the second variation, ${}^a\mathbf{Z}$ is *generalized* to contain the identity wherever translational freedoms occur, with the remainder of the definition the same, as follows:

$$ \mathbf{Z} = \begin{bmatrix} \ddots & & \\ & \mathbf{I}_3 \quad \mathbf{0} & \\ & \mathbf{0} \quad {}^a\mathbf{Z} & \\ & & \ddots \end{bmatrix} \tag{3.35} $$

The results from Eq. (3.30) are added only to each *rotational* block of stiffness; only freedoms belonging to *single node* are coupled by (3.30).

3.2.1.6. Implications for General Finite Element Analysis

Since there is, in principal, no restriction on the form of the potential defined by (3.25), what was developed in the last subsections applies also to C^0 finite elements that can be expressed as a function of unit shell normals at the nodes. Referring to Steps 1) through 4) in Section 2, we note that no modifications to the sequence of calculations are necessary, provided that

1) The unit vector positions are calculated using the deformational *rotation operators* directly, rather than first converting to pseudovector angles, as is done with the corotational implementation in STAGS. The modification to the software to meet this objective is trivial.

2) The *linearization* defined by (3.26) through (3.31) should be carried out. In most situations, it means only computing the symmetrized version of (3.30) and adding this 3 x 3 contribution to each rotational block. The additional computational load is very small compared with the existing implementation of relations like (3.28).

3) The *update formula* for rotations must be modified to conform with Eq. (3.11). This has been done, and proves to be simple, stable, and efficient.

3.2.2. The Function of a Pseudovector

Although the results from Section 3.2.1 can be carried intact to many C^0 elements whose rotational freedoms can be described by unit vectors attached to each node, there are many other elements inherited from moderate rotation theory that use angles *directly in the element interpolation*. For the SH410 family in STAGS, there are three *independent* rotations at each node. For the ordinary addition rule for small rotation composition, no inconsistency exists (and true Newton convergence is observed), but the elements are restricted at most to moderate rotations. When the corotational theory was implemented, the correct *objective* method of updating rotations was invoked as

$$ {}^{a}\mathbf{S}_{(k+1)} = \Delta {}^{a}\mathbf{S}_{(k+1,k)} {}^{a}\mathbf{S}_{(k)} \tag{3.1} $$

where we have repeated Eq. (3.1) for emphasis. With the introduction of (3.1), the consistency is lost, and so is the efficiency of the convergence to the solution. We now investigate what is really going on during a Newton iteration, and introduce a sample problem to check it out.

3.2.2.1. The Linearization Process

In all iteration algorithms, the goal is to obtain *solution increments* that bring a current configuration into a new configuration that satisfies equilibrium requirements, and to do this in as few iterations as possible. Our measure of satisfaction of equilibrium is the *residual*, or some vector function $\mathbf{f}(\mathbf{x}_{(i)})$ that *vanishes* when we are done. The sequence of events is stated in Eqs. (3.13). Note that when convergence is taking place, $\mathbf{f}$ is very small. Let us assume that near equilibrium we have

$$ \mathbf{f}_{(i)} = \epsilon \dot{\mathbf{f}}_{(i)} \tag{3.36} $$

where $\dot{\mathbf{f}}$ is the *directional derivative* of the internal force with respect to the *parameter* ϵ, with ϵ some tiny constant that vanishes when equilibrium is satisfied. We also have shortened the notation, so that the system state information subscripted to $\mathbf{f}_{(i)}$ means of course, $\mathbf{f}(\mathbf{x}_{(i)})$. We wish to solve

$$ \mathbf{K}\Delta\mathbf{x}_{(i)} = -\epsilon \dot{\mathbf{f}}_{(i)} \tag{3.37} $$

for some small value of ϵ. We see, however, that on the one hand, the update of the system rotations follows (3.1) instead of (3.13), so we have, using (3.11),

$$\mathbf{S}_{(i+1)} = \exp(\epsilon[\dot{\omega}_S]_{(i)})\mathbf{S}_{(i)} \tag{3.38}$$

where $[\dot{\omega}_S]$ is also intrepreted as the *directional derivative* of the rotational part of $\mathbf{x}$ with respect to the parameter ϵ and is the outcome of the solution of (3.37). Clearly the increments depend on ϵ because of (3.37), vanishing as the residual vanishes. On the other hand, if the *element* strain energy depends instead on *angles* instead of ${}^a\mathbf{D}_{(i)}$ (see Section 2), we must connect this variation with the what happens in (3.38) as ϵ vanishes. Suppose we express ${}^a\mathbf{D}_{(i)}$ as an exponential of the pseudovector that we use in the element calculations:

$${}^a\mathbf{D}_{(i)} = \exp([\boldsymbol{\theta}_D]_{(i)}) \tag{3.39}$$

Now, presuming the element frame remains fixed, the variation in the relative rotation ${}^a\mathbf{D}_{(i)}$ is

$$\begin{aligned} \delta\,{}^a\mathbf{D}_{(i)} &= [\delta\boldsymbol{\omega}_S]_{(i)}\,{}^a\mathbf{D}_{(i)} \\ &= \epsilon[\dot{\omega}_S]\,{}^a\mathbf{D}_{(i)} \end{aligned} \tag{3.40}$$

which is from (2.12). In the limit of small ϵ, the difference between two surface triads computed by (3.38) is identical to (3.40). Taking the variation of (3.39) and comparing this with (3.40) we have

$$\delta\{\exp([\boldsymbol{\theta}_D]_{(i)})\} = [\delta\boldsymbol{\omega}_S]_{(i)}\mathbf{D}_{(i)} \tag{3.41}$$

Noting the equivalence of the solution increments through (3.38), we wish to solve for $[\delta\boldsymbol{\omega}_S]_{(i)}$, as follows:

$$[\delta\boldsymbol{\omega}_S] = \delta\{\exp([\boldsymbol{\theta}_D]_{(i)})\}\mathbf{D}_{(i)}^T \tag{3.42}$$

What we need then is the derivative of the exponential of a skew-symmetric matrix times its transpose, or

$$\frac{d\exp([\boldsymbol{\theta}])}{d\epsilon}\exp(-[\boldsymbol{\theta}]) \tag{3.43}$$

for any skew-symmetric $[\boldsymbol{\theta}]$ dependent on some parameter ϵ. If we have this connection, we have consistency with the update procedure in (3.38).

This missing link has been provided us by SIMO in [9], which, when translated to the normalization in [7], is described by the relation

$$\frac{d\exp([\boldsymbol{\theta}])}{d\epsilon}\exp(-[\boldsymbol{\theta}]) = \frac{[\dot{\bar{\boldsymbol{\theta}}}] + \frac{1}{2}([\bar{\boldsymbol{\theta}}][\dot{\bar{\boldsymbol{\theta}}}] - [\dot{\bar{\boldsymbol{\theta}}}][\bar{\boldsymbol{\theta}}])}{1 + \frac{1}{4}|\bar{\boldsymbol{\theta}}|^2} \tag{3.44}$$

where the normalization in [7] is

$$\bar{\boldsymbol{\theta}} = \frac{\tan(|\boldsymbol{\theta}|/2)\boldsymbol{\theta}}{|\boldsymbol{\theta}|/2} \tag{3.45}$$

and where in both (3.44) and (3.45) the dots over the symbols represent derivatives with respect to the parameter ϵ. The axial vector equivalent of (3.45) is

$$\dot{\omega} = \frac{\dot{\bar{\theta}} + \frac{1}{2}\bar{\theta} \times \dot{\bar{\theta}}}{1 + \frac{1}{4}|\bar{\theta}|^2} \tag{3.46}$$

where we have taken note of (3.42), and assumed that $\delta\omega$ is a function of ϵ. We have dropped system state indices for the moment. Eq. (3.46) is the link we are looking for to complete the linearization for elements like the SH410. We next must invert (3.46) to express $\dot{\bar{\theta}}$ as a function of $\dot{\omega}$, the subject of the next subsection.

3.2.2.2. The Inversion of the Exponential Derivative

It is tedious, but straightforward to invert (3.46). First, we express the inverse as

$$\dot{\bar{\theta}} = \alpha\dot{\omega} + \beta\bar{\theta} \times \dot{\omega} + \gamma(\bar{\theta} \cdot \dot{\omega})\bar{\theta} \tag{3.47}$$

because the vectors $\dot{\omega}$, $\bar{\theta} \times \dot{\omega}$, and $\bar{\theta}$ certainly span the 3 x 3 space described by (3.46). If we substitute (3.47) into (3.46), we must get the identity. This is true only for

$$\begin{aligned} \alpha &= 1 \\ \beta &= -\frac{1}{2} \\ \gamma &= \frac{1}{4} \end{aligned} \tag{3.48}$$

To get to this point, we had to make repeated and careful use of relations (3.5). The final formula we want is

$$\dot{\bar{\theta}} = \dot{\omega} - \frac{1}{2}\bar{\theta} \times \dot{\omega} + \frac{1}{4}(\bar{\theta} \cdot \dot{\omega})\bar{\theta} \tag{3.49}$$

3.2.2.3. The Linearization of a Function of $\bar{\theta}$

We are now in the position to linearize a potential that is a function of $\bar{\theta}$. Suppose we have such a potential defined by

$$U = U({}^1\bar{\theta}, {}^2\bar{\theta}, \cdots, {}^N\bar{\theta}) \tag{3.50}$$

with the indices ranging over "nodes" 1 to N, exactly like the definition of the potential in (3.25). Letting the new "internal forces" be defined by the relation

$${}^a\bar{f} = \frac{\partial U}{\partial {}^a\bar{\theta}} \tag{3.51}$$

we have, using (3.49), the relations

$$\begin{aligned} \delta^a\omega^T{}^a\mathbf{f} &= \delta^a\bar{\boldsymbol{\theta}}^T{}^a\bar{\mathbf{f}} \\ &= \delta^a\omega^T\{{}^a\bar{\mathbf{f}} + \frac{1}{2}{}^a\bar{\boldsymbol{\theta}} \times {}^a\bar{\mathbf{f}} + \frac{1}{4}({}^a\bar{\boldsymbol{\theta}} \cdot {}^a\bar{\mathbf{f}}){}^a\bar{\boldsymbol{\theta}}\} \end{aligned} \tag{3.52}$$

Thus the internal forces derived from angles are modified by

$${}^a\mathbf{f} = {}^a\bar{\mathbf{f}} + \frac{1}{2}{}^a\bar{\boldsymbol{\theta}} \times {}^a\bar{\mathbf{f}} + \frac{1}{4}({}^a\bar{\boldsymbol{\theta}} \cdot {}^a\bar{\mathbf{f}}){}^a\bar{\boldsymbol{\theta}} \tag{3.53}$$

Great care must be taken since the order of the operations used to derive (3.52) is important. Close examination will show that the *transpose* of (3.49) is used for the consistent linearization.

The second derivative is obtained by differentiating (3.53) and using (3.49) again. This is complicated but straightforward to yield

$$\begin{aligned} \mathbf{K}_{mat} &= \mathbf{Z}^T\bar{\mathbf{K}}\mathbf{Z} \\ {}^a\mathbf{K}_{geom} &= -\frac{1}{2}[{}^a\bar{\mathbf{f}}]{}^a\mathbf{Z} + \frac{1}{4}\{({}^a\bar{\boldsymbol{\theta}} \cdot {}^a\bar{\mathbf{f}}){}^a\mathbf{Z} + {}^a\bar{\boldsymbol{\theta}}\ ({}^a\bar{\mathbf{f}}^T{}^a\mathbf{Z})\} \end{aligned} \tag{3.54}$$

where each 3 x 3 block of ${}^a\mathbf{Z}$ is defined by

$${}^a\mathbf{Z} = \mathbf{I}_3 - \frac{1}{2}[{}^a\bar{\boldsymbol{\theta}}] + \frac{1}{4}{}^a\bar{\boldsymbol{\theta}}\ {}^a\bar{\boldsymbol{\theta}}^T \tag{3.55}$$

Of course, (3.55) is just the matrix equivalent of (3.49), as can be seen from Eq. (2.13).

3.2.2.4. The Question of Symmetry

Note the similarity to (3.28) through (3.31) that define the linearization of a function of a unit vector. This shows that there is a strong link between functions of a unit vector and functions of the pseudovector $\bar{\boldsymbol{\theta}}$. The "geometric" stiffness is again, in general, nonsymmetric, just as for the function of the unit vector. It can be shown by direct substitution and comparison with (3.53) that once again the stiffness matrix becomes symmetric according to the relation (3.34). Thus all we have said about questions of convergence for conservative systems also applies here.

3.2.2.5. The Test with a Trial Potential

In order to test what we have come up with, we went through all the steps described by Eqs. (3.53) through (3.55) with the simple quadratic potential

$$U(\bar{\boldsymbol{\theta}}) = \frac{1}{2}(\bar{\boldsymbol{\theta}} - \bar{\boldsymbol{\theta}}_0)^T\bar{\mathbf{K}}(\bar{\boldsymbol{\theta}} - \bar{\boldsymbol{\theta}}_0) \tag{3.56}$$

where $\bar{\mathbf{K}}$ is a 3 x 3, symmetric, positive-definite matrix input by the user, and where $\bar{\boldsymbol{\theta}}_0$ is some constant starting value of the pseudovector completely equivalent to some "applied"

loads. Except for the relations stated in this section, the trial software was the same as for the function of the unit vector. We included the option to symmetrize the stiffness, or to use its transpose. In contrast to the previous program, we could start with the nodal triad $\mathbf{S}_{(0)}$ in any conceivable orientation, enabling us to have the most general set of initial conditions.

The results were gratifying. No matter what the initial state, and no matter what the input stiffness was, after a very few iterations, the convergence was quadratic, showing once again the complete consistency of the linearization. Any tinkering with relations (3.53) through (3.55), such as omitting some terms that may be considered small like those quadratic in $\bar{\boldsymbol{\theta}}$ completely destroyed the quadratic convergence to the solution. However, the symmetrized matrix produced the identical favorable convergence behavior, as did its transpose. The solution was insensitive to the initial state except when the pseudovector was computed for angles near 180°, where it is known to be singular. This is of no consequence to ordinary finite element analysis, because, of course, the angles we are speaking of are the local, small, *relative* rotations for which only moderate rotation theory need apply.

It is therefore clear that this linearization is complete, and that what was said about functions of a unit vector carries over intact to functions of a pseudovector. In particular, the symmetrized version of the stiffness works for any conservative system. The band structure of the matrix $\mathbf{Z}$ is described by Eq. (3.35). Only freedoms connected to a single node are coupled by $\mathbf{K}_{geom}$. The basic matrix operations are identical for the two cases. The only real fundamental difference is that here, for the pseudovector $\bar{\boldsymbol{\theta}}$, we can have *three* independent freedoms per node, as the submatrices described here can, in general, be rank 3. This is also gratifying, because elements using the pseudovector such as the SH410 can have three independent rotations with finite stiffness.

3.2.3. Functions of Angles

Up to this point, we have assumed the element rotations could be described by $\bar{\boldsymbol{\theta}}$, which has the tangent normalization described in [7] and by (3.45). What happens if we use real angles? By real angles, we mean that if one rotates about a fixed axis by a certain angle, the magnitude of the pseudovector will agree with this angle. We shall call this pseudovector $\boldsymbol{\theta}$; it is this quantity that appears in Eq. (3.39) for the exponential of the skew-symmetric matrix. We discuss the linearization next.

3.2.3.1. Linearization of a Function of Angles

The equivalent of (3.46) for $\boldsymbol{\theta}$ is also taken from [9]:

$$\dot{\boldsymbol{\omega}} = \frac{\sin|\boldsymbol{\theta}|}{|\boldsymbol{\theta}|}\dot{\boldsymbol{\theta}} + \left(1 - \frac{\sin|\boldsymbol{\theta}|}{|\boldsymbol{\theta}|}\right)\left(\frac{\boldsymbol{\theta}\cdot\dot{\boldsymbol{\theta}}}{|\boldsymbol{\theta}|}\right)\frac{\boldsymbol{\theta}}{|\boldsymbol{\theta}|} + \frac{1}{2}\left(\frac{\sin(|\boldsymbol{\theta}|/2)}{|\boldsymbol{\theta}|/2}\right)^2 \boldsymbol{\theta}\times\dot{\boldsymbol{\theta}} \qquad (3.57)$$

This was unappetizing to invert, but can be done using the methods developed in the previous sections. The inverse is

$$\begin{aligned}\dot{\boldsymbol{\theta}} &= \dot{\boldsymbol{\omega}} - \frac{1}{2}\boldsymbol{\theta}\times\dot{\boldsymbol{\omega}} + g\boldsymbol{\theta}\times(\boldsymbol{\theta}\times\dot{\boldsymbol{\omega}}) \\ &= (1-g|\boldsymbol{\theta}|^2)\dot{\boldsymbol{\omega}} - \frac{1}{2}\boldsymbol{\theta}\times\dot{\boldsymbol{\omega}} + g(\boldsymbol{\theta}\cdot\dot{\boldsymbol{\omega}})\boldsymbol{\theta}\end{aligned} \tag{3.58}$$

where

$$g(|\boldsymbol{\theta}|) = \frac{\sin(|\boldsymbol{\theta}|/2) - (|\boldsymbol{\theta}|/2)\cos(|\boldsymbol{\theta}|/2)}{|\boldsymbol{\theta}|^2\sin(|\boldsymbol{\theta}|/2)} \tag{3.59}$$

The matrix equivalent of (3.58) is

$${}^a\mathbf{Z} = (1-g|{}^a\boldsymbol{\theta}|^2)\mathbf{I}_3 - \frac{1}{2}[{}^a\boldsymbol{\theta}] + g\,{}^a\boldsymbol{\theta}\,{}^a\boldsymbol{\theta}^T \tag{3.60}$$

where we have added the node designation a for clarity.

Using the same arguments as before, we have for the internal forces the relation

$${}^a\mathbf{f} = {}^a\bar{\mathbf{f}} + \frac{1}{2}{}^a\boldsymbol{\theta}\times{}^a\bar{\mathbf{f}} + g\,{}^a\boldsymbol{\theta}\times({}^a\boldsymbol{\theta}\times{}^a\bar{\mathbf{f}}). \tag{3.61}$$

relating the old internal forces ${}^a\bar{\mathbf{f}}$ to the new ${}^a\mathbf{f}$.

It is straightforward but very tedious to derive the second variation, as follows:

$$\begin{aligned}\mathbf{K}_{mat} &= \mathbf{Z}^T\bar{\mathbf{K}}\mathbf{Z} \\ \mathbf{K}_{geom} &= -\frac{1}{2}[{}^a\mathbf{f}]\,{}^a\mathbf{Z} + g\{({}^a\boldsymbol{\theta}\cdot{}^a\bar{\mathbf{f}})\,{}^a\mathbf{Z} + {}^a\boldsymbol{\theta}\,({}^a\bar{\mathbf{f}}^T\,{}^a\mathbf{Z}) - 2\,{}^a\bar{\mathbf{f}}\,({}^a\boldsymbol{\theta}^T\,{}^a\mathbf{Z})\} \\ &\quad + \frac{g'}{|{}^a\boldsymbol{\theta}|}\{{}^a\boldsymbol{\theta}\times({}^a\boldsymbol{\theta}\times{}^a\bar{\mathbf{f}})\}\,\{{}^a\boldsymbol{\theta}^T\,{}^a\mathbf{Z}\}\end{aligned} \tag{3.62}$$

where the derivative of g is expressed as

$$\frac{g'}{|{}^a\boldsymbol{\theta}|} = \frac{\phi(\phi+\sin\phi\cos\phi) - 2\sin^2\phi}{16\phi^4\sin^2\phi} \tag{3.63}$$

with the definition

$$\phi = \frac{|{}^a\boldsymbol{\theta}|}{2} \tag{3.64}$$

Note that this linearization is more complicated than that involving the pseudovector with the tangent normalization. g' requires special treatment for small angles, accomplished by using a power series expansion. All that was said before applies here, except for the additional complications in (3.61) through (3.64).

3.2.3.2. Testing with an Example Potential

We used the same potential as in the last section, but this time interpreting the pseudovector as "angles" requiring the linearization just introduced. Here, in contrast to the last problem, there is a special case where the answer comes out in just *one* iteration. If one begins with the *identity* as the initial nodal triad (and some nonzero $\boldsymbol{\theta}_0$), the increments produced solve this quadratic potential exactly. When these increments are turned into a surface triad, and that triad multiplies the starting value (the identity), we are left with something that, when inverted, reproduces the same angles that were solved for in the first place. Obviously, for this special case, one iteration is sufficient. On the other hand, any other starting position converts the linear problem in $\boldsymbol{\theta}$ to a nonlinear problem (because rotations neither add nor commute). This problem converges quadratically regardless of the starting state to the correct solution. Convergence was absolutely insensitive to any nonzero starting position.

As before, the stiffness can be easily shown to be symmetric when equilibrium is satisfied, and, as before, the solution takes place at the same rate whether the stiffness is symmetrized or not. It is to be noted that the "super convergence" obtained by identity as the starting state *requires* a symmetrized stiffness, because only then does the contribution from $\mathbf{Z}$ vanish and the linear problem is retrieved. At this point, we decided to try a problem with fixed moments to see what effect this nonconservative external force had on the solution. In this case, of course, the skew-symmetric part of the stiffness does not vanish, but instead is proportional to one half the external moments. As expected, we obtained the rapid, quadratic convergence *only* when the *unsymmetric* stiffness was used. Otherwise, the convergence was linear at best. We note here in passing that unless

$$\mathbf{m} \cdot \delta\boldsymbol{\theta} \times \delta\boldsymbol{\phi} = \mathbf{0} \tag{3.65}$$

where $\mathbf{m}$ is the unbalanced moment and where $\delta\boldsymbol{\theta}$, $\delta\boldsymbol{\phi}$ are two independent allowable variations of the rotational freedoms, the forcing is nonconservative. This result is from [9], but it has appeared in the literature many times. From (3.65), any boundary condition that restrains *only one* rotation is not conserving, whereas a free edge and a boundary allowing only one free rotation are conservative. One can visualize why the boundary with the single rotational constraint is nonconserving with the following argument:

1) Consider the freedom in the x direction as forbidden, *i.e.* no rotation about that axis can take place.
2) Now rotate about the z axis 90° (allowed), followed by a rotation of some θ about the y axis. Then rotate the result back by $-90°$ about the z axis again.
3) The result is a rotation by θ about the forbidden x direction!

Certainly, less extreme angles lead to similar results; this boundary is path-dependent and therefore nonconservative. ARGYRIS [1,2] has treated this subject at length, from which he derived his conserving semi-tangential rotations and symmetric geometric stiffnesses. The problem of nonconservative boundaries will come back to haunt us in succeeding sections.

3.2.3.3. Implications for General Finite Element Analysis

The arguments in subsection 3.2.1.6 also apply here. The generality of what we have derived makes these results immediately applicable to the finite element code that uses elements that depend explicitly on pseudovectors with either the tangent normalization, or normalized as angles. As before, no modifications to the sequence of calculations are necessary, provided that

1) The local element pseudovectors have normalization consistent with the choice of linearization from Section 3.2.2 or 3.2.3.

2) The modifications to the linearization described above are implemented. Note that the band structure and coupling are exactly as in the case of the potential as a function of unit vectors. The additional computational effort is the same as before.

3) The *update formula* for rotations is the exponential of a pseudovector normalized as angles, just as in the case of the unit vector potential. The modification we had for the C^0 elements works here, too.

Whereas for the unit vector case (C^0 elements), the right hand side remains unchanged from what exists now, for elements that depend on angles like the 410, *the right hand side is altered*. This is, of course, unsettling. Fortunately, the grids required for reasonable convergence usually imply small local element angles. In that case, ${}^a\mathbf{Z}$ approaches the identity, and the right hand side as modified differs little from the original. Convergence with respect to discretization remains intact. On the other hand, the corrections here certainly enhance such convergence, allowing for coarser grids and hence potential substantial savings in computational and manpower costs. And, as we shall see, the *faster, more stable* convergence to the solution will yield further benefits, including the possibility of solving problems heretofore impossible because of poor convergence.

3.3. Final Steps in the Linearization

We are almost ready to put all this together into a working package, and demonstrate improved convergence for the corotational implementation. But first, since we know that the elements as now configured only approximately obey local equilibrium in the deformed configuration, we must come to terms with the effect of the projection operator $\mathbf{P}$ on the *second variation*. By utilizing the *global* invariance properties of the geometric stiffness, we will be able to account for all or almost all of the effect of the variation of $\mathbf{P}$ and the local element frame.

3.3.1. The Behavior of the System under Rigid Rotation

If the *coordinate frame* is rotated by a given *infinitesimal* angle $-\delta\boldsymbol{\omega}$, internal and boundary forces of the system will appear to rotate by $+\delta\boldsymbol{\omega}$. The relation, from Eq. (3.4) is

$$\delta\,{}^a\mathbf{f} = \delta\boldsymbol{\omega} \times {}^a\mathbf{f}$$

But the stiffness matrix is the first order term in the Taylor expansion of the internal force, so that certainly

$$\begin{aligned}\mathbf{K}(\boldsymbol{\phi}\cdot\boldsymbol{\omega}) &= \{\cdots, \boldsymbol{\omega}\times {}^a\mathbf{f}_{tr}, \boldsymbol{\omega}\times {}^a\mathbf{f}_r, \cdots\}^T \\ &= -\{\cdots, [{}^a\mathbf{f}_{tr}], [{}^a\mathbf{f}_r], \cdots\}^T\boldsymbol{\omega} \\ &= -[\mathbf{F}]\boldsymbol{\omega}\end{aligned} \tag{3.66}$$

where the symbol $[\mathbf{F}]$ denotes a long column vector consisting of a 3 x 3 skew-symmetric matrix for the translational ${}^a\mathbf{f}_{tr}$ and the rotational ${}^a\mathbf{f}_r$ internal forces for each node a in the system. Here the left superscripts denote node numbers, and $\boldsymbol{\phi}$ is the infinitesimal rotation vector as defined in Section 2. We know that such a rotation is not conserving, because moments fixed in space also rotate, and because rotations do not commute. We shall see the implications of this in the next section.

3.3.2. The End Run: the Completion of the Linearization

Let us for the moment suppose we knew in advance the *true* tangent stiffness, and call this one $\hat{\mathbf{K}}$. From the definition of the projector

$$\mathbf{P} = \mathbf{I} - \boldsymbol{\phi}\boldsymbol{\gamma}^T$$

we can "solve" for the identity

$$\mathbf{I} = \mathbf{P} + \boldsymbol{\phi}\boldsymbol{\gamma}^T \tag{3.67}$$

and pre- and postmultiply the stiffness to yield

$$\hat{\mathbf{K}} = (\mathbf{P}^T + \boldsymbol{\gamma}\boldsymbol{\phi}^T)\hat{\mathbf{K}}(\mathbf{P} + \boldsymbol{\phi}\boldsymbol{\gamma}^T) \tag{3.68}$$

Multiplying this out, we have

$$\hat{\mathbf{K}} = \mathbf{P}^T\hat{\mathbf{K}}\mathbf{P} + \boldsymbol{\gamma}\boldsymbol{\phi}^t\hat{\mathbf{K}}\mathbf{P} + \mathbf{P}^T\hat{\mathbf{K}}\boldsymbol{\phi}\boldsymbol{\gamma}^T + \boldsymbol{\gamma}\boldsymbol{\phi}^T\hat{\mathbf{K}}\boldsymbol{\phi}\boldsymbol{\gamma}^T \tag{3.69}$$

We invoke (3.66) to yield

$$\hat{\mathbf{K}} = \mathbf{P}^T\hat{\mathbf{K}}\mathbf{P} - \boldsymbol{\gamma}[\mathbf{F}]^T\mathbf{P} - \mathbf{P}^T[\mathbf{F}]\boldsymbol{\gamma}^T - \boldsymbol{\gamma}[\mathbf{F}]^T\boldsymbol{\phi}\boldsymbol{\gamma}^T \tag{3.70}$$

The first term on the right hand side can be identified as the "material" stiffness with the "true" stiffness replaced with the one we have calculated and projected with $\mathbf{P}$ as

$$\mathbf{K} = \mathbf{P}^T\bar{\mathbf{K}}\mathbf{P} \tag{3.71}$$

where $\bar{\mathbf{K}}$ results from ordinary finite element computations. The *approximate* version of (3.70) becomes

$$\hat{\mathbf{K}} = \mathbf{K} - \boldsymbol{\gamma}[\mathbf{F}]^T\mathbf{P} - \mathbf{P}^T[\mathbf{F}]\boldsymbol{\gamma}^T - \boldsymbol{\gamma}[\mathbf{F}]^T\boldsymbol{\phi}\boldsymbol{\gamma}^T \tag{3.72}$$

Note that the added terms depend only on the internal forces. We started out with a symmetric matrix and assumed that by invoking the global rotation properties, we would

end up with a symmetric matrix. We see, however, that by reintroducing the definition of $\mathbf{P}$ we get instead

$$\hat{\mathbf{K}} = \mathbf{K} - \gamma[\mathbf{F}]^T - [\mathbf{F}]\gamma^T + \gamma\phi^T[\mathbf{F}]\gamma^T \tag{3.73}$$

which cannot be symmetric unless the 3 x 3 matrix

$$\mathbf{K}_{red} = \phi^T[\mathbf{F}] \tag{3.74}$$

is also symmetric. Using the properties (3.66) we find a contradiction: the matrix is unsymmetric, which means (3.66) describes an nonconservative system. We now take a cue from [1], and assume that the moments rotate *half* as much as the forces. This is what he calls the "semi-tangential" moment; his geometric stiffnesses rotate the forces by $-[\bar{\mathbf{F}}]$, where

$$[\bar{\mathbf{F}}]^T = \{\cdots, [{}^a\mathbf{f}_{tr}], \frac{1}{2}[{}^a\mathbf{f}_r], \cdots\} \tag{3.75}$$

It can be shown directly that $\mathbf{K}_{red}$ is symmetric when $[\bar{\mathbf{F}}]$ replaces $[\mathbf{F}]$, provided the element internal forces are self-equilibrated. Since the projector $\mathbf{P}$ enforces local equilibrium with respect to the deformed configuration, this requirement is *always* satisfied, so that $\mathbf{K}_{red}$ is symmetric, as is the total tangent stiffness.

To summarize the operations, we begin by calculating the ordinary, consistent tangent stiffness $\bar{\mathbf{K}}$, including the parts of the linearization derived in Sections 3.2 that apply to the particular situation (such as for C^0 elements as a function of a unit vector, for example). We also calculate the consistent internal force, also using the consistent linearization. Only then do we apply the projector to both the internal force and stiffness (see Eq. (3.71)). The internal forces are divided into two classes. For each *set* of translational freedoms, they are arranged into a skew-symmetric array, and placed into their proper position in $[\bar{\mathbf{F}}]$. Then *half* the rotational internal forces are likewise arranged and placed into their proper place in $[\bar{\mathbf{F}}]$. We calculate the symmetric matrix

$$\mathbf{K}_{red} = \phi^T[\bar{\mathbf{F}}] \tag{3.76}$$

and then the total tangent stiffness by

$$\hat{\mathbf{K}}_{tan} = \mathbf{P}^T\bar{\mathbf{K}}\mathbf{P} - \gamma[\bar{\mathbf{F}}]^T - [\bar{\mathbf{F}}]\gamma^T + \gamma\mathbf{K}_{red}\gamma^T \tag{3.77}$$

3.4. The Proof in the Pudding: Testing in the STAGS Code

With all the pieces in place, we are in the position to implement the new theory in a full-blown finite element code. At this time, only one element, the often-used SH410 was tried. Software for the linearization of the element energy as a function of a pseudovector was extremely simple to implement, involving a very small amount of programming. Existing utilities carried us the bulk of the way. The operations to construct $\mathbf{P}$ and to implement (2.18) and the first term in (3.77) was in place from the linear work in Section 2, except that we had to pass *deformed* coordinates instead of *undeformed* nodal positions into the

various calculations for the projector. The remaining terms in (3.77) required only a little additional effort.

Our first test was to produce the numerically-differentiated tangent stiffness and compare it with our calculated version. When we did, we got poor agreement! When we ran the same as a test case, the solution converged only linearly, even with true Newton selected as the solution option. The printed numerical stiffness was still unsymmetric, just as before. But right away we noticed that we had used as our external load *consistent line loads* derived from moderate rotation theory. These loads involve moments about fixed axes. What we have said about nonconservative systems certainly applies here: a quick check on the stiffness demonstrated that it was out of symmetry by *exactly half* the unsatisfied external moments.

We repeated the runs with another problem with conserving boundaries and fixed point loads. Immediately, the numerically-calculated stiffness became symmetric. The calculated stiffness agreed to within 5 orders of magnitude (relative to the principal diagonals) of the stiffness calculated by finite difference. Finally, and most important, we regained the true Newton quadratic convergence for the entire solution history, including when the structure was highly deformed and collapsed (past the limit point). Some small differences were seen between certain stiffness terms, a subject to be pursued later with the total derivative of the projection operator. We will then hope to show that the result will be almost, if not exactly, what we have derived here. One must note that unless *all* steps are included in the linearization, the good convergence is lost. This includes the modifications to the corotational software described in Sections 3.2.1.6 and 3.2.3.3. For the STAGS 410 element, the linearization consistent with the corotational implementation described in [7] is with the pseudovector with the *tangent* normalization. This means, in particular, the use of relations (3.53), (3.54), (3.55), and taking note of the band structure (3.35), carrying out the operation in (3.28) with the value of ${}^a\mathbf{Z}$ from (3.55). Any terms left out because of assumed "smallness" eventually destroy the quadratic convergence for solutions in the large deformation range.

The next runs were made using the normalization of the pseudovector as angles. After linking to routines that produce the appropriate linearization, the convergence was just as good, and so were the answers. No real difference was observed between the two sets of runs.

It is hard at this point to gauge what effect this will have on the ordinary, garden variety analysis. We have shown already that there is no *profound* difference in the overall converged solution. This is good, because it means that the corotational theory as it stood was adequate for most situations. This fact has been buttressed by a multitude of runs that have been completed satisfactorily. On the other hand, having a consistent linearization is interesting in its own right. Even if benefits to the ordinary user are not dramatic, confidence that the solution is consistently derived is comforting, especially since the *right hand side* is also modified, both through the projector $\mathbf{P}$ and the linearization of the pseudovector (for elements like 410). One can certainly foresee cases where convergence previously was difficult, and therefore solution impossible with things the old way. In particular, when taking advantage of the new Thurston Equivalance Transformation processor (ET) [11] to carry a solution through bifurcation in the presence of modal inter-

action, a consistent tangent stiffness can be crucial. The modifications to the right hand side from the projector or for functions of a pseudovector required for the SH410 element will also be important when calculating the higher-order terms needed to properly account for the modal interaction; the combined effect of an inconsistent tangent and approximate higher-order terms could put the solution in jeopardy. We anticipate experimenting with collapse and bifurcation problems that were difficult in the past to see if consistency will gain us the robustness to overcome the complicated deformations characteristic of these structures.

To this point, we have demonstrated that even for the *modified Newton* solution strategy, we get a ratio of about .85 in the iteration count as compared to 1 for the old way when just the projector is introduced. Since element-related computation accounts for the bulk of the work for these simple problems, there is a net *loss* in overall efficiency, with a ratio of about 1.1. When the very inexpensive additions to the linearization are added, the ratio of iterations drops to about .65, with the work level to about .95 for some simple cases. If the iteration ratio holds up, for large problems where matrix operations tend to dominate (none of these were altered in any way), we may approach a gain of .65 to one in efficiency, measured as relative time spent doing the calculations. These results were computed using a simple, but nontrivial, small problem. For those problems that are intrinsically difficult, the difference may be between success and failure. In the case of true Newton, its status has been restored as a robust method of solution for conservative problems defined by an elastic potential. Before, true Newton cost may times more than modified Newton. For this small case, the factor was reduced to about 1.5, which of course will be much greater for large problems; true Newton is always expensive because we must factor *every iteration*.

3.5. Extending the Conservative Boundary Condition

The one messy aspect of things as they now stand is the possibility of the user generating a nonconservative forcing or boundary condition without knowing it. Certainly, if one has true follower forces or localized nonconserving pressure loads, one cannot expect to avoid the consequences. For pressure loads derived from a potential, we are in good shape, because a *load stiffness* is introduced to include the effects of the change in direction of the pressure load. The implementation in STAGS is not affected by what we have derived here.

For other types of load, we have a problem. We have already discussed how troublesome boundaries can be. Loads determined by moments fixed in space caused delays in the research presented here. Fortunately, the solution to these problems is already implied by Eq. (3.56). There is a term in that equation of the form

$$\boldsymbol{\theta}^T \bar{\mathbf{K}} \boldsymbol{\theta}_0 = \boldsymbol{\theta}^T \mathbf{m} \tag{3.78}$$

where certainly $\mathbf{m}$ could be interpreted as an *external moment*. But (3.78) is a potential, a function of a well-defined, unique pseudovector with, in this case, the angle normalization. Therefore, (3.61) through (3.64) apply. What one gets is a modification to the applied load, as expected. In addition, however, we get the new *load stiffness* terms (3.62). All

angles of course would be based on the relative rotation the affected node has undergone from its resting state (${}^a\mathbf{S}_{(i)}$). One only has to show that the external load defined in this way is consistent with those cases that satisfy (3.65). But (3.65) states basically the moment must follow the direction of the rotational freedom variation. In practice, this means that either the moment is zero, or that rotation is possible only about a single axis. If the moment is zero, (3.62) contributes nothing. If the rotation is permitted to take place about a *single* axis, one can immediately see by examining (3.58) that

$$\boldsymbol{\theta} \times \dot{\boldsymbol{\omega}} = \mathbf{0}$$

because only one direction is permitted, and hence

$$\dot{\boldsymbol{\theta}} = \dot{\boldsymbol{\omega}} \tag{3.79}$$

Therefore, no further transformations are needed, and the *usual interpretation of the external load survives*. Note that because of the scalar terms in (3.53), such correspondence is *impossible* when the tangent pseudovector is selected.

For follower nodal loads, we have available only the contribution to the residual, as follows:

$$\begin{aligned} {}^a\mathbf{f}_{tr} &= {}^a\bar{\mathbf{f}} \\ {}^a\mathbf{f}_r &= \mathbf{0} \end{aligned} \tag{3.80}$$

where ${}^a\bar{\mathbf{f}}$ is a given nodal follower load rigidly attached to the nodal triad. The load stiffness is derived directly from (3.79), (3.4), and (2.13):

$$\mathbf{K}_{geom} = \begin{bmatrix} \mathbf{0} & -[{}^a\bar{\mathbf{f}}] \\ \mathbf{0} & \mathbf{0} \end{bmatrix} \tag{3.81}$$

This matrix is unsymmetric for all cases because the follower load is nonconservative.

3.5.1. Application to Arc-Length Solution Algorithms

One important constraint condition to be considered arises whenever continuation parameter solution procedures are invoked. In these procedures, the load parameter is cast as *dependent* variable to be solved for along with the displacements. Typically, the additional constraint equation is a function of some "arc length" along an approximate tangent to the solution path, often approximated by the relation

$$\mathbf{t}^T(\mathbf{u}_{(i)} - \mathbf{u}_{(0)}) + t_\lambda(\lambda_{(i)} - \lambda_{(0)}) - \Delta\eta = 0 \tag{3.82}$$

where $\mathbf{u}_{(i)}$ are the displacements of the *current iterate* i, where (0) refers to the latest *converged* solution (*iteration 0*), and where $\mathbf{t}$ is an approximate "tangent" to the current solution path. Here, λ is the load factor and t_λ is that component of $\mathbf{t}$ belonging to the *load factor*, and $\Delta\eta$ is the arc step length (independent variable) selected beforehand.

The problem with (3.82) is that the difference between the displacement states is not valid for *rotational freedoms* when the arc step is large, as can be the case for a fine-tuned algorithm. Fortunately, we can bring the results of the previous sections to bear on the constraint equation if we *redefine* (3.82) as follows:

$$\mathbf{t}_{tr}^T(\mathbf{u}_{(i)} - \mathbf{u}_{(0)}) + \mathbf{t}_r^T\boldsymbol{\theta}(\mathbf{R}) + t_\lambda(\lambda_{(i)} - \lambda_{(0)}) - \Delta\eta = 0 \tag{3.83}$$

where

$$\mathbf{R} = \mathbf{S}_{(i)}\mathbf{S}_{(0)}^T \tag{3.84}$$

is the relative rotation from the reference state 0 to the current iterate i. Note that again we have redefined the system state subscripts to refer to *iteration count*, with 0 as the reference converged solution. If we define $\boldsymbol{\theta}$ by the relation

$$\exp([\boldsymbol{\theta}]) = \mathbf{R} \tag{3.85}$$

then (3.83) reverts to (3.82) for small angles. Following the arguments in Sect. 3.2.2, we see that Eq. (3.44) or (3.57) applies, where this time $\boldsymbol{\theta}$ is the appropriate pseudovector corresponding to the *relative rotation* $\mathbf{R}$ through Eq. (3.85).

One must evaluate (3.83) and its first derivative to complete the arc-length calculations. To evaluate (3.83), the relative rotation is calculated from (3.84) and used to obtain $\boldsymbol{\theta}$ (3.85) by standard means. Either the angle or tangent normalization can be used. The derivative of (3.83) is treated just like the right hand side of (3.78), from which a modified "internal force" is extracted through the use of (3.53) as follows:

$${}^a\mathbf{t}_m = {}^a\mathbf{t} + \frac{1}{2}{}^a\bar{\boldsymbol{\theta}} \times {}^a\mathbf{t} + \frac{1}{4}({}^a\bar{\boldsymbol{\theta}} \cdot {}^a\mathbf{t}){}^a\bar{\boldsymbol{\theta}} \tag{3.86}$$

for the pseudovector $\bar{\boldsymbol{\theta}}$ with tangent normalization corresponding to $\boldsymbol{\theta}$ in (3.85). For angle normalization, we proceed using (3.61) instead. In either case, ${}^a\mathbf{t}_m$ replaces $\mathbf{t}$ in the arc-length extended stiffness for the rotational freedoms pertaining to node a. The rest of the calculations are unchanged.

4. *Summary and Conclusions*

In this work, we have succeeded in largely completing the element-independent corotational formulation introduced in [7]. We have demonstrated that the theory as it has existed up to now is incomplete. We have uncovered these deficiencies and derived what is necessary to fill the gaps in the theory. Sample problems were introduced that cover the relevant points, and what was derived was tested on these problems. The linearization of a potential as a function of a unit vector, or of a pseudovector with two kinds of normalization was shown to be completely consistent, with true Newton, quadratic convergence to solution. Finally, the parts were put together in the large structural analysis code STAGS and superior convergence was demonstrated. Extensions to follower loads and unconservative boundaries were derived.

This work culminates a long effort to realize the full potential of the element-independent corotational theory. As originally posed, such a theory would greatly promote a host of inexpensive finite elements to robust performance for difficult nonlinear collapse problems. The roadblocks have been fundamental element inconsistencies (such as nonsastisfaction of equilibrium) and the accompanying poor convergence properties. Two important gaps have now been filled:

1) The element is automatically *self-equilibrated*, even if in its original conception local equilibrium was not satisfied.

2) The linearization is *consistent*.

What we have not done is fill in such holes as rank-deficiency, distortion sensitivity in a plane, or shear locking. But we envision that perhaps elements could be defined without concern for frame invariance, something to be enforced by the methods developed here. Perhaps trigonometric functions could once again be used as shape functions for shell elements? Finally, if it could be possible to define the element interpolation *entirely* as a function of scalars defined by inner products of the unit nodal normals and the displacement vectors taken in proper combination, frame invariance would be *guaranteed*, and no added "corotational" theory would be necessary. What we have here provides the recipe for the linearization of these elements also.

5. *Suggestions for Future Research*

The most immediate need is to test thoroughly what we have already in place. We wish to see if more difficult problems can now be tackled. Following this, careful benchmarks should be run to measure what immediate gains in solution efficiency have been realized. In addition, the sensitivity of solutions to the order, sequence, and frequency of the element frame update should be investigated to see whether moderate rotation theory within the local element environment is in effect. If it proves true that the solution is insensitive to the frequency of the element frame update, strategies for taking advantage of this should be investigated. Provision for the *two* normal rotations in the special SH411 elements should be made before any of this work is implemented for that element.

Before publishing the complete linearization including the derivative of projection operator, we wish to calculate *all* derivatives analytically, using symbolic manipulation on the computer. Following the completion of that effort, attention should be paid to the nonconserving boundaries and external loads.

Areas of new research abound. For example, we mentioned elements as a function of fundamental relative scalar quantities that are already frame-invariant. Trigonometric shape functions could be exhumed, and their use as shape functions should be examined in the light of what we can do now. Elements completely lacking invariance to rotation or translation could be used with the generalized projection operator (the translational part is trivial) to exploit the otherwise favorable behavior they might have.

6. *References*

1. J. H. Argyris et al, "Finite Element Method - the Natural Approach", *Comp. Meths. in Appl. Mech. and Engrg.* **17/18** (1979) 1-106.

2. J. H. Argyris, "An Excursion into Large Rotations," *Comp. Meth. in Appl. Mech. and Engrg.* **32** (1982) 85-155.

3. C. K. Mak, "Finite Element Analysis of Buckling and Post-Buckling Behavior of Arches with Geometric Imperfections," *J. Comp. Struct.*, (1972).

4. D. Kang, "Hybrid Stress Finite Element Method," Ph.D. Thesis, MIT, June 1986

5. K. C. Park and G. M. Stanley, "A Curved C^0 Shell Element Based on Assumed Natural-Coordinate Strains," *J. Applied Mechanics*, June, 1986.

6. K. C. Park, G. M. Stanley, and D. L. Flaggs, "A Uniformly Reduced, Four Noded C^0 Shell Element with Consistent Rank Corrections", *Comp. & Struct.*, 1985.

7. C. C. Rankin and F. A. Brogan, "An Element-Independent Corotational Procedure for the Treatment of Large Rotations," *ASME J. Pressure Vessel Technology* **108** pp. 165-174 (May, 1986)

8. J. Simo, "A Finite Strain Beam Formulation. Three-Dimensional Dynamic Problem, Part I," *Computer Meth. in Appl. Mech. & Engng.* **49**, pp. 55-70 (1985)

9. J. Simo and L. Vu Quoc, "Three Dimensional Finite Strain Rod Model, Part II: Computational Aspects," *Memorandum No. UCB/ERL M85/31* Electronics Research Laboratory, College of Engineering, U. Calif. Berkeley, (April, 1985).

10. G. M. Stanley, "Continuum-Based Shell Elements," Ph.D. Thesis, Stanford, August 1985.

11. G. A. Thurston, F. A. Brogan, and P. Stehlin, "Postbuckling Analysis Using a General Purpose Code," *AIAA Journal* **24**, No. 6, pp. 1013-1020 (June, 1986).

12. B. F. De Veubeke, "The Dynamics of Flexible Bodies," *Int. J. Engng. Sci.* **14** (1976) 895-913.

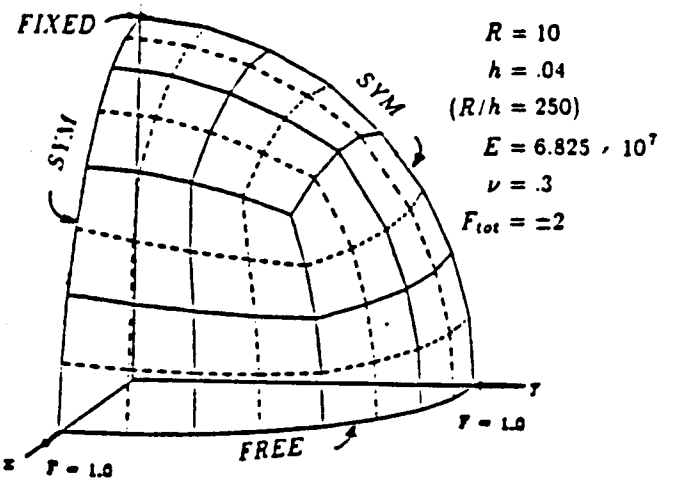

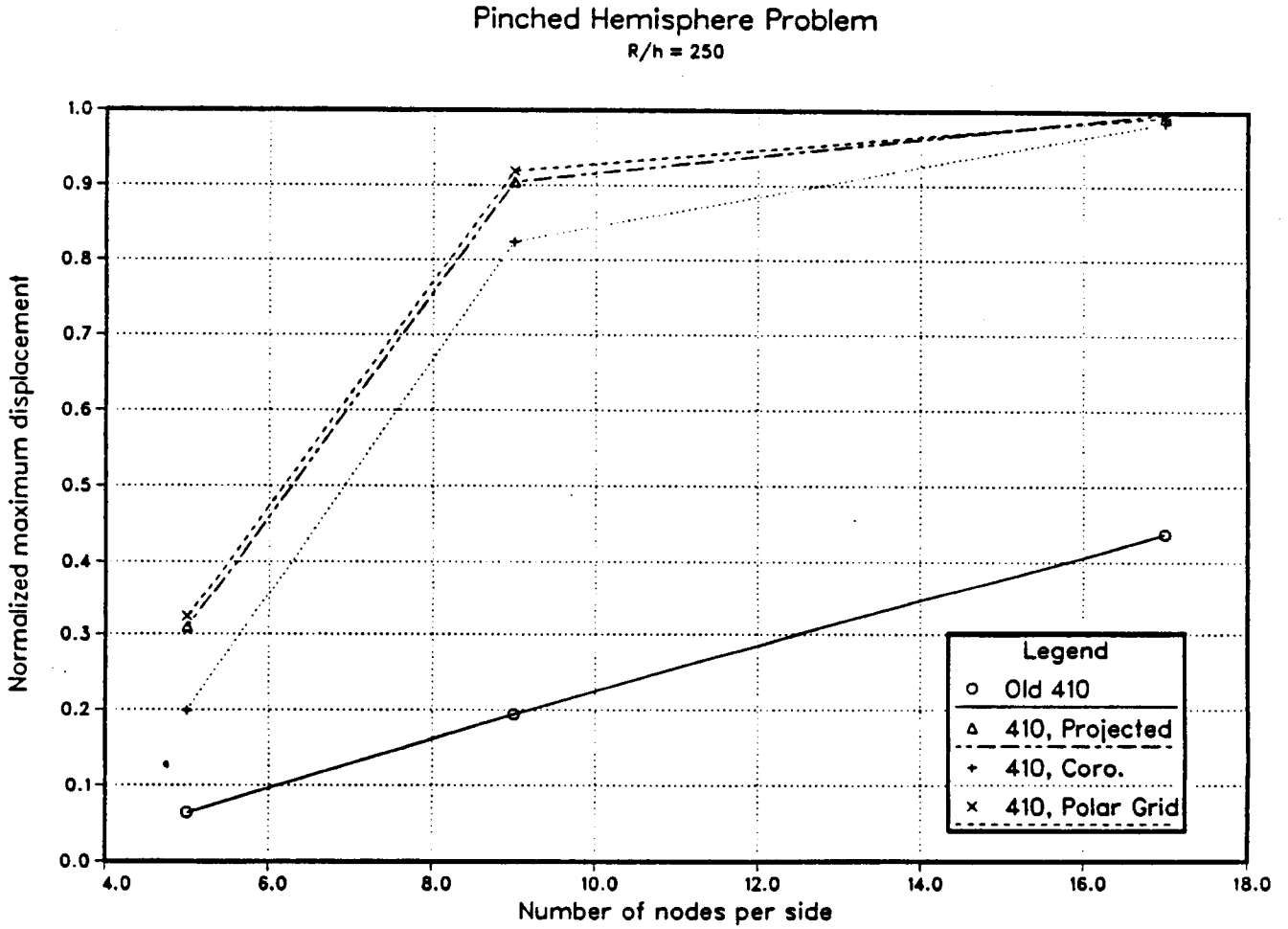

Figure 1. Pinched hemisphere results for linear and nonlinear analysis with SH410

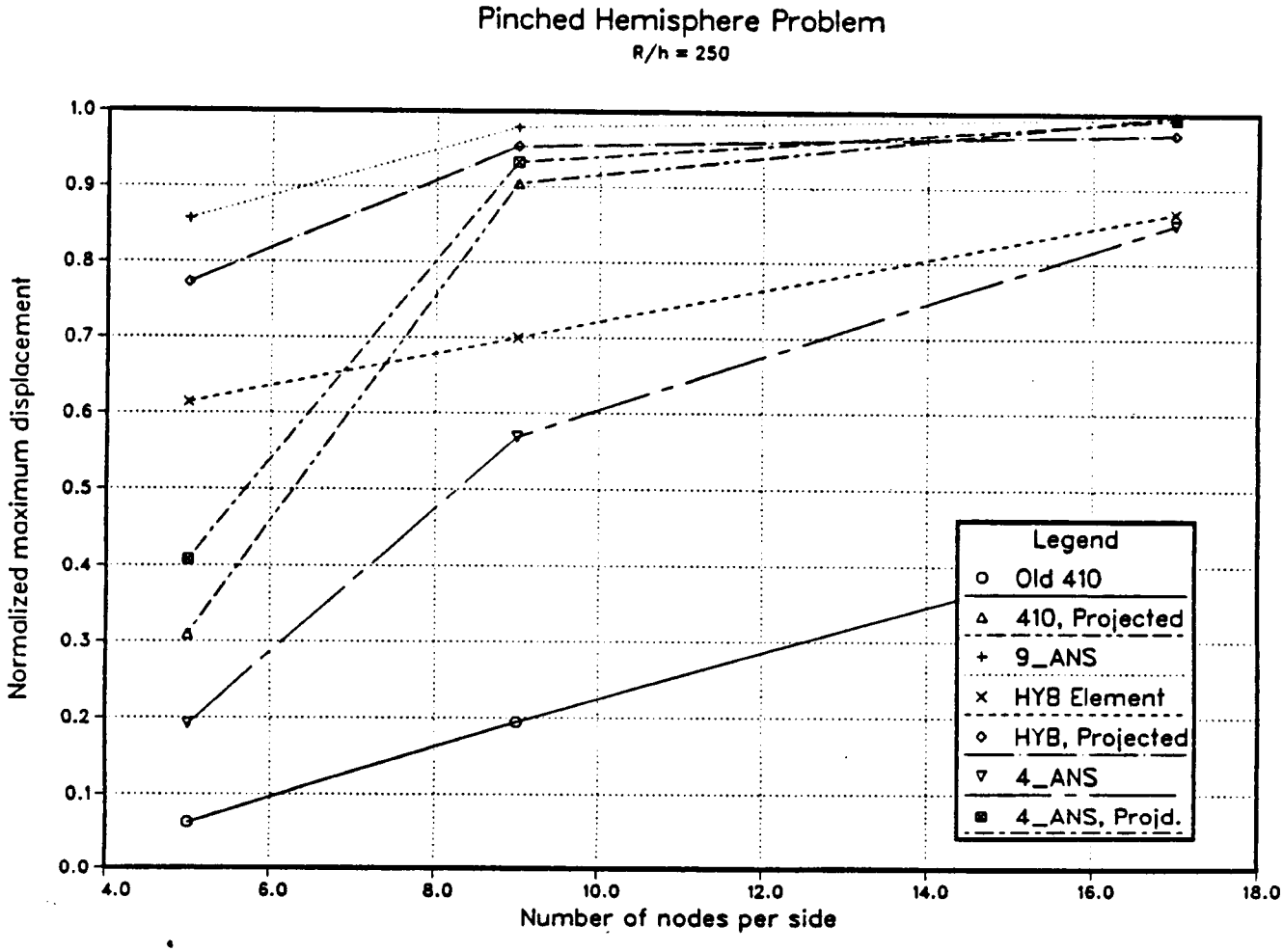

Figure 2. Pinched hemisphere results for various elements with and without P

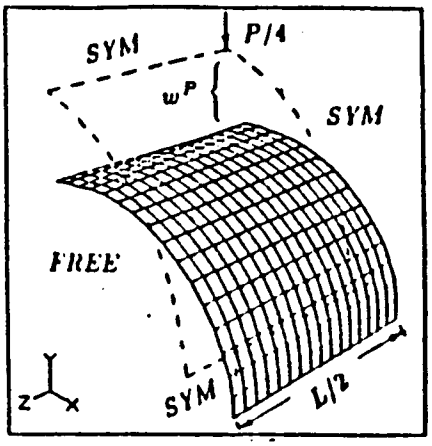

$E = 10.5 \times 10^6$
$\nu = .3125$
$R = 4.953$
$L = 10.35$

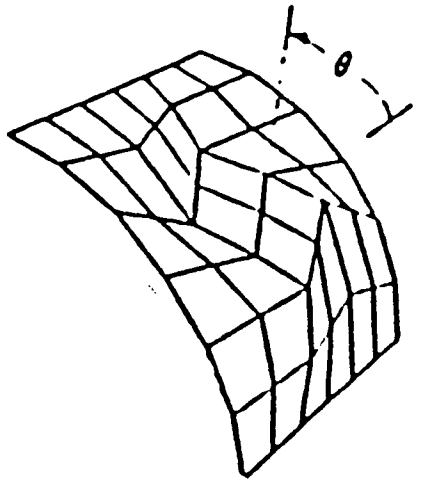

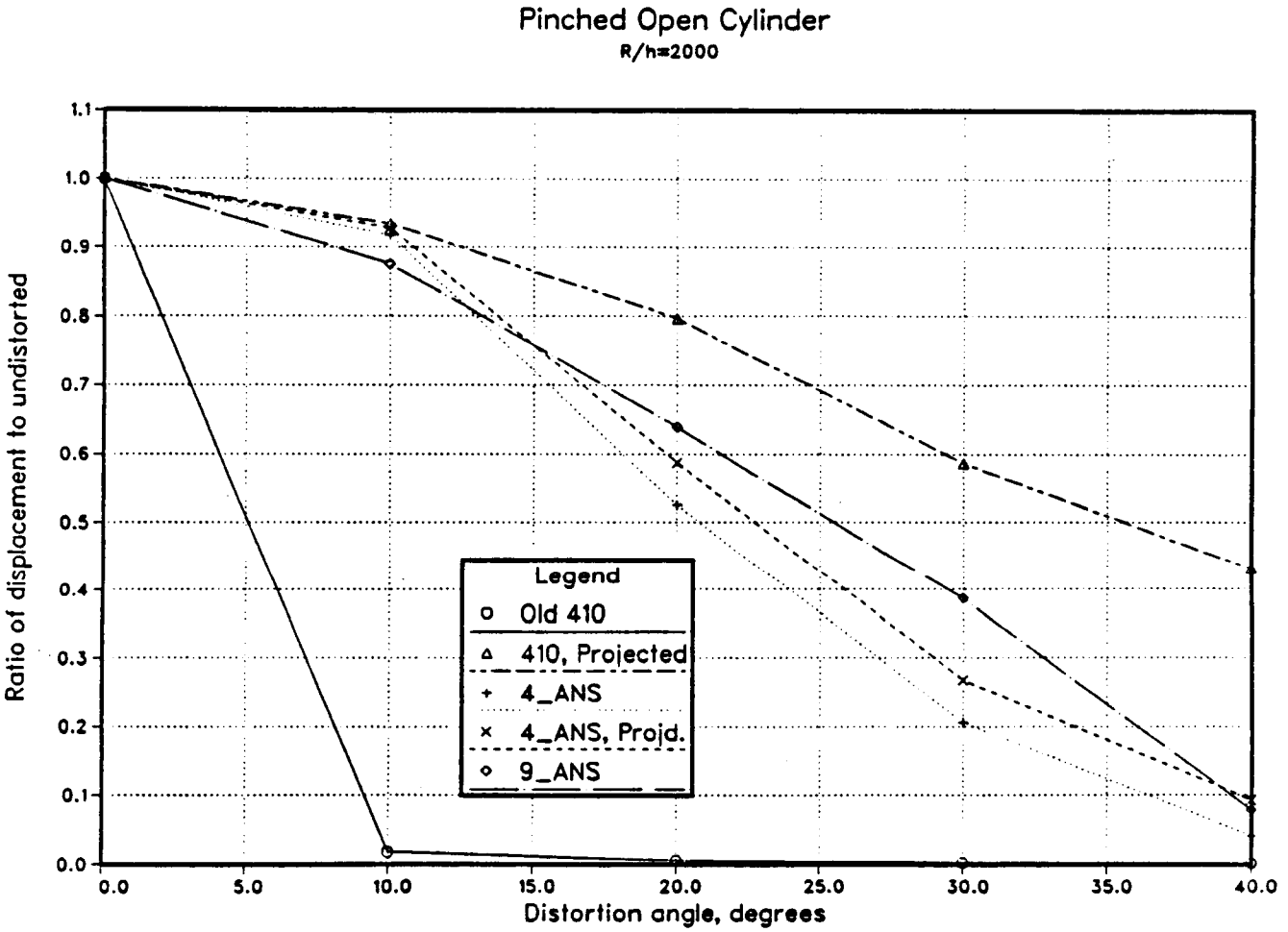

Figure 3. Pinched cylinder results for various elements with and without P

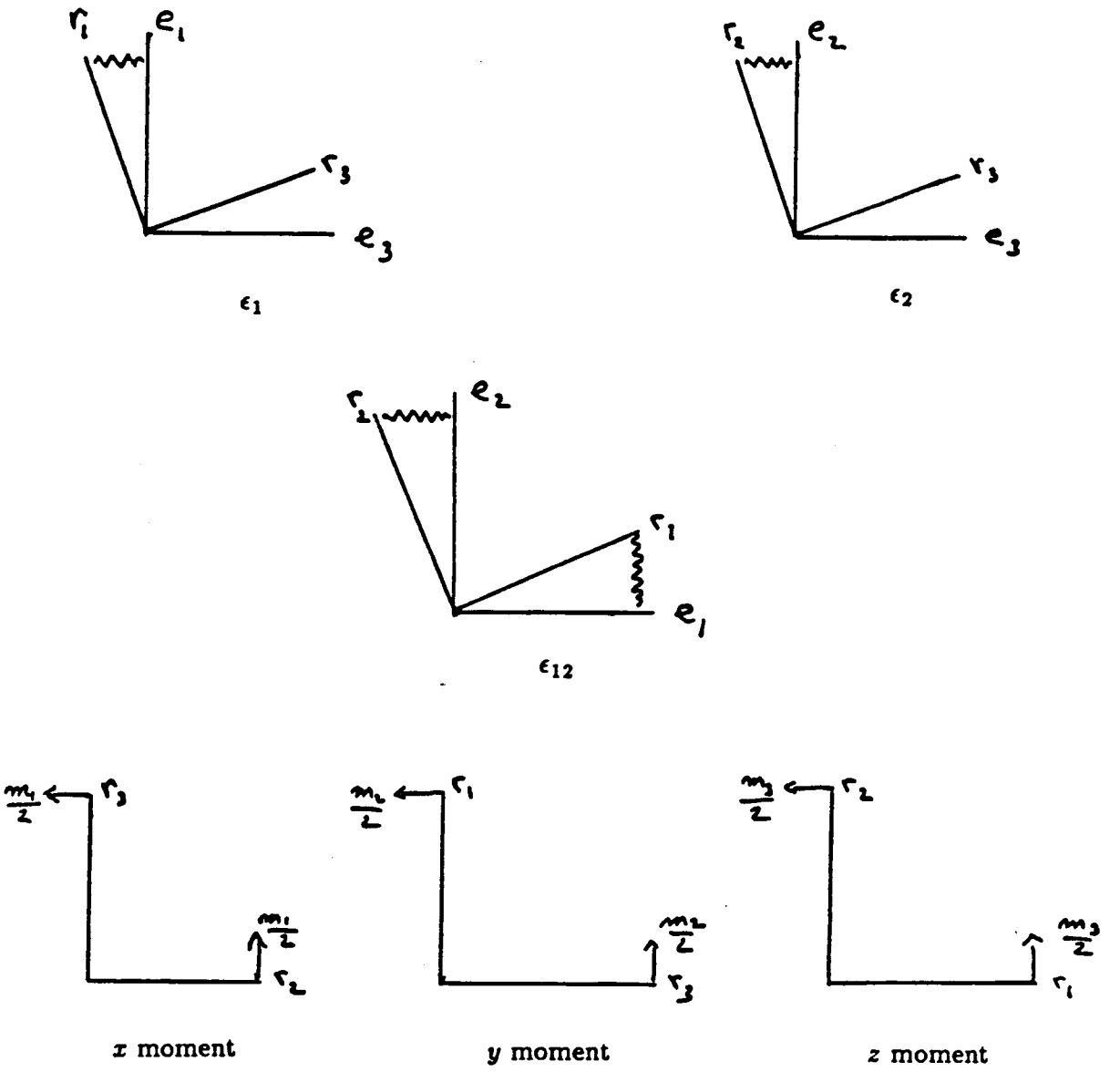

Figure 4. Illustration of example function of unit vectors

NASA
National Aeronautics and Space Administration

Report Documentation Page

1. Report No.	2. Government Accession No.	3. Recipient's Catalog No.
NASA CR-178418		

4. Title and Subtitle
Consistent Linearization of the Element-Independent Corotational Formulation for the Structural Analysis of General Shells

5. Report Date
Jan. 1988

6. Performing Organization Code

7. Author(s)
Charles C. Rankin

8. Performing Organization Report No.
LMSC-F202439

10. Work Unit No.
505-63-11-03

9. Performing Organization Name and Address
Computational Mechanics Section
Lockheed Palo Alto Research Laboratory
Palo Alto, CA 94304

11. Contract or Grant No.
NAS1-18101

13. Type of Report and Period Covered
Contractor Report

12. Sponsoring Agency Name and Address
National Aeronautics and Space Administration
Langley Research Center
Hampton, VA 23665-5225

14. Sponsoring Agency Code

15. Supplementary Notes
Langley Technical Monitor: Gaylen A. Thurston
Task 5 Final Report

16. Abstract

A consistent linearization is provided for the element-independent corotational formulation, providing the proper first and second variation of the strain energy. As a result, the warping problem that has plagued flat elements has been overcome, with beneficial effects carried over to linear solutions. True Newton quadratic convergence has been restored to the Structural Analysis of General Shells (STAGS) code for conservative loading using the full corotational implementation. Some implications for general finite element analysis are discussed, including what effect the automatic frame invariance provided by this work might have on the development of new, improved elements.

17. Key Words (Suggested by Author(s))	18. Distribution Statement
Consistent Linearization Element-Independent Corotational Formulation Shells	Unclassified - Unlimited Subject Category 39

19. Security Classif. (of this report)	20. Security Classif. (of this page)	21. No. of pages	22. Price
Unclassified	Unclassified	51	